9-1-2023

Ceramic particles reinforced copper matrix composites manufactured by advanced powder metallurgy: Preparation, performance, and mechanisms

Yi-Fan Yan

Shu-Qing Kou

Hong-Yu Yang

Shi-Li Shu

Feng Qiu

See next page for additional authors

10.1088/2631-7990/acdb0b

Yan, Y. F., Kou, S. Q., Yang, H. Y., Shu, S. L., Qiu, F., Jiang, Q. C., & Zhang, L. C. (2023). Ceramic particles reinforced copper matrix composites manufactured by advanced powder metallurgy: Preparation, performance, and mechanisms. International Journal of Extreme Manufacturing, 5(3), article 032006. https://doi.org/10.1088/2631-7990/acdb0b

TOPICAL REVIEW • OPEN ACCESS

Ceramic particles reinforced copper matrix composites manufactured by advanced powder metallurgy: preparation, performance, and mechanisms

To cite this article: Yi-Fan Yan *et al* 2023 *Int. J. Extrem. Manuf.* **5** 032006

OPEN ACCESS
IOP Publishing | IMMT
International Journal of Extreme Manufacturing
Int. J. Extrem. Manuf. **5** (2023) 032006 (35pp)
https://doi.org/10.1088/2631-7990/acdb0b

Topical Review

Ceramic particles reinforced copper matrix composites manufactured by advanced powder metallurgy: preparation, performance, and mechanisms

Yi-Fan Yan[1,2], Shu-Qing Kou[1,2], Hong-Yu Yang[1,2,5,*], Shi-Li Shu[1,3,*], Feng Qiu[1,2,*], Qi-Chuan Jiang[1,2] and Lai-Chang Zhang[4,*]

[1] State Key Laboratory of Automotive Simulation and Control, Jilin University, Renmin Street No.5988, Changchun, Jilin Province 130025, People's Republic of China
[2] Key Laboratory of Automobile Materials, Ministry of Education and Department of Materials Science and Engineering, Jilin University, Renmin Street No. 5988, Changchun, Jilin Province 130025, People's Republic of China
[3] School of Mechanical and Aerospace Engineering, Jilin University, Renmin Street No. 5988, Changchun, Jilin Province 130025, People's Republic of China
[4] Centre for Advanced Materials and Manufacturing, School of Engineering, Edith Cowan University, 270 Joondalup Drive, Joondalup, Perth, Western Australia 6027, Australia
[5] School of Materials Science and Engineering, Jiangsu University of Science and Technology, Zhenjiang 212003, People's Republic of China

E-mail: yanghongyu2021@jlu.edu.cn, shushili@jlu.edu.cn, qiufeng@jlu.edu.cn and lczhangimr@gmail.com

Received 21 December 2022, revised 27 March 2023
Accepted for publication 31 May 2023
Published 22 June 2023

Abstract

Copper matrix composites doped with ceramic particles are known to effectively enhance the mechanical properties, thermal expansion behavior and high-temperature stability of copper while maintaining high thermal and electrical conductivity. This greatly expands the applications of copper as a functional material in thermal and conductive components, including electronic packaging materials and heat sinks, brushes, integrated circuit lead frames. So far, endeavors have been focusing on how to choose suitable ceramic components and fully exert strengthening effect of ceramic particles in the copper matrix. This article reviews and analyzes the effects of preparation techniques and the characteristics of ceramic particles, including ceramic particle content, size, morphology and interfacial bonding, on the diathermancy, electrical conductivity and mechanical behavior of copper matrix composites. The corresponding models and influencing mechanisms are also elaborated in depth. This review contributes to a deep

* Authors to whom any correspondence should be addressed.

2631-7990/23/032006+35$33.00

understanding of the strengthening mechanisms and microstructural regulation of ceramic particle reinforced copper matrix composites. By more precise design and manipulation of composite microstructure, the comprehensive properties could be further improved to meet the growing demands of copper matrix composites in a wide range of application fields.

Keywords: copper matrix composites, advanced powder metallurgy, model prediction, particle characteristics, strengthening mechanism

1. Introduction

Copper (Cu) and its alloys are indispensable functional materials in modern industry. Cu exhibits superior thermal conductivity (398 W $(m{\cdot}K)^{-1}$ at 25 °C) among metals, which makes it the material of choice for heat-conducting components, including electric packaging materials and heat sinks. Meanwhile, the high electrical conductivity (5.8×10^7 S m^{-1} at 25 °C) of Cu makes Cu and its alloys widely used in wires, bus bars, transformer windings, heavy-duty motors, telephone wires and telephone cables. Combined with its good corrosion resistance and friction performance, Cu is also widely used in the field of electric brush, pantograph skateboard, brakes and wet clutches [1–4]. However, the high density (8.9 g cm^{-2}), low strength, low hardness and undesirable wear resistance of Cu cannot meet the demand for lightweight and efficient functional materials [5–7]. For example, Cu would delaminate from silicon wafer and squeeze the chip due to its high coefficient of thermal expansion (CTE) in the field of electronics. This would shorten the service life of electrical devices and cause damage to precision instruments.

Recently, the Cu matrix composites doped with ceramic particles demonstrate excellent mechanical properties and thermophysical characteristics; such excellent performance of the Cu matrix composites could broaden the applications of Cu matrix composites as functional materials [8, 9]. The high specific elastic modulus and hardness, high-temperature stability, together with low density and CTE of ceramic particles make up for the deficiency of Cu in mechanical properties and high temperature service performance. Compared to pure Cu, the ceramic reinforced Cu matrix composites show superior mechanical strength, high wear resistance and low CTE [10, 11]. Particularly, the high-temperature stability of Cu matrix composites could be greatly enhanced by introducing ceramic phases. However, ceramic particles, especially nano-scaled particles, tend to agglomerate in the Cu matrix due to their large specific areas and van der Waals forces. Furthermore, the poor wettability between ceramic phase and Cu matrix combined with the susceptibility of ceramic particles to surface contamination can result in weak interfacial bonding between these phases [12–14]. The weakened interface could downgrade the overall performance of the composites. In the past decades, research in this field has focused on obtaining uniformly dispersed ceramic particles in the matrix and on rationally designing and manipulating the composite microstructure. On this basis, considerable endeavors [15–18] have been made to obtain ceramic reinforced Cu matrix composites with excellent comprehensive properties, such as preparation processes, pretreatment of raw materials, and so on. Generally, manipulating the microstructure of composites, especially the content, size, distribution and morphology of ceramic particles and interfacial bonding, is an effective way to further improve the comprehensive performance of ceramic reinforced Cu matrix composites [19–21]. As a rule, the preparation technique is one of decisive factors in obtaining high-performance composites by manipulating the characteristics of the ceramic phases and the microstructure of composites [10, 22–24]. Casting, powder metallurgy, melt infiltration, friction stir processing, etc are widely used to prepare ceramic reinforced Cu matrix composites. Among these preparation technologies, powder metallurgy is most widely used to prepare Cu matrix composites. This process can flexibly select reinforcing particles with various types, sizes and morphologies, and it mitigate the reaction between the ceramic particles and the matrix owing to the special molding method of powder metallurgy (under the solid state or semi-liquid state). Most importantly, powder technology is more beneficial to control the distribution of ceramic particles, which gives full play to their strengthening effect. Therefore, it is well worth investigating the influence of powder metallurgy techniques and microstructure manipulation on the properties of ceramic reinforced Cu matrix composites, to lay a foundation for further enhancing Cu matrix composites in the future.

As such, this article reviews the preparation by advanced powder technology and the effects of the content, size and morphology of ceramic particles as well as the particle-matrix interface on the properties of Cu matrix composites. Meanwhile, the effects of preparation processes and ceramic characteristics on Cu matrix composites are derived from a vertical comparison of results from the same literature. Due to the lack of comparability between different ceramic types caused by small differences in experimental raw materials, equipment, operating procedures and other factors, this article does not overview the effect of ceramic type on the composites. Further applications of Cu matrix composites and the strengthening mechanism of ceramic particles in the composites are systematically elaborated. Based on the manipulative link between the microstructure and the comprehensive properties in the ceramic particles reinforced Cu matrix composites, this article also discusses the improvement direction and future development prospects of the preparation process and microstructure optimization for ceramic particles reinforced Cu matrix composites.

2. Advanced powder metallurgy techniques for fabricating Cu matrix composites

Powder metallurgy is one of the earliest techniques used to prepare Cu matrix composites. This preparation process starts with fully mixing the Cu powder, reinforcing phase powder and additives in a certain proportion to form a uniform composite powder. Then, the Cu matrix composites are obtained by pressing and sintering under certain pressure and temperature. For example, Zhang *et al* [25] successfully synthesized $Zr_2Al_3C_4$ particles reinforced Cu matrix composite by this way at 850 °C and 35 MPa pressure. The $Zr_2Al_3C_4$/Cu composite demonstrates comparable electrical conductivity and higher strength compared to the Cu/graphite composite. However, the low compactness and poor interfacial bonding significantly downgrade the comprehensive properties of powder metallurgical products. The unsatisfactory dispersion of the ceramic particles in the Cu matrix is also a drawback of the composite prepared by powder metallurgy. In order to further enhance the strengthening effect of ceramic reinforced Cu matrix composites prepared by powder metallurgy, more advanced techniques were proposed in regard to the powder mixing, sintering process, raw material pretreatment and other special processes. Among all these advanced techniques, mechanical alloying, spark plasma sintering, internal oxidation and *in-situ* processing (as shown in figure 1) are superior in terms of powder mixing, sintering process, raw material pretreatment and special processes, respectively. These preparation processes are conducive to further improving the dispersion of ceramic particles in the Cu matrix and the interfacial bonding between the ceramic phase and the Cu matrix. Besides, higher compactness and more effective microstructure control are achieved in the composites through these preparation processes [26–28]. Therefore, this section focuses on the optimization of powder metallurgy by mechanical alloying, spark plasma sintering, internal oxidation and *in-situ* processing to prepare Cu matrix composites with superior performance.

2.1. Mixing technique

For the powder metallurgy technique, the mixing of powders is the key step to obtain Cu matrix composites with good dispersity and high compactness. In the process of powder mixing, the conventional method can only obtain the uniform dispersion powders through powder mixer, and the resulting powders remain loose and are prone to agglomeration [31]. In contrast, mechanical alloying optimizes the bonding and the dispersion between the powders during the mixing process [32]. It is well known that mechanical alloying, as an atomic alloying technique, utilizes the mechanical energy generated by high-energy ball mill to make the composite powders repeatedly deformed and broken under the action of high-speed rotating grinding balls. In regard to preparing the dispersion-strengthened alloys and composites, mechanical alloying is conducive to the interatomic diffusion of each component and the enhancement of interfacial bonding strength, thereby obtaining a high strengthening effect [33–36]. As shown in figure 2(a), ductile particles (e.g. metal matrix) are deformed and broken by the collision of grinding balls and eventually flattened; by contrast, brittle particles (e.g. ceramic particles) are quickly crushed. Subsequently, a lamellar composite structure is formed by alternating the flake ductile powder and the brittle powder; that is, brittle powders are distributed at the joins of ductile layers. After further ball milling, the distance between the ductile and brittle powders becomes smaller, and eventually the composite powders are mixed and curled [37, 38].

Figures 2(b)–(f) show the TEM images of composite powders at different milling time [39]. When the milling time is short (1 h and 5 h), the agglomerated ceramic powders can still be clearly observed. As increasing the milling time (10 h), the particle agglomeration is alleviated, as shown in figure 2(c). Furthermore, some ceramic powders have been welded with the Cu powders. Further increasing the milling time facilitates a uniform distribution of reinforced particles and dissipation of agglomerated powders. The grain size of Cu matrix decreases as increasing the milling time and reaches the minimum at a certain state [41]. Figures 2(g)–(k) show the TEM images of composite powders with different ceramic contents [40]. The sizes of particles and the agglomerated powders decrease significantly as increasing the ceramic content and the particle size reaches 45.4 nm for those nanocomposites containing 12 wt.% ceramic phase. Generally, cold-welding causes an increase in particle size, while the fracture of flakes results in the reduction in particle size [42]. The existence of hard particles leads to an increase in local deformation of Cu matrix near ceramic particles, which enhances the work hardening rate of the matrix. The increased work hardening rate is beneficial to increase the fracture of flakes. Moustafa and Taha [9] prepared the nano-sized ceramic particles reinforced Cu matrix nanocomposites with excellent comprehensive properties through mechanical alloying. The introduction of nano-sized ceramic particles triggers severe plastic deformation and grain refinement during mechanical alloying. As the content of ceramic particles in composites increases, the grain size of the Cu matrix further decreases, while both the dislocation density and microstrain of the Cu matrix increase.

In addition to powder factors and milling time, the ball-to-powder weight ratio (BPR) and the rotation speed (in rpm) also significantly affect the properties of dispersion-strengthened composites. Wang *et al* [43] successfully prepared TiC dispersion strengthened copper composite by a two-step ball milling process, and they systematically evaluated the effects of ball milling processes on the properties of Cu matrix composites. During this process, Ti and graphite were first ball milled and then Cu powder was added. Under the condition of high BPR together with high rotation speed, Ti and C can be completely converted to TiC, which led to higher electrical conductivity but lower strength of the composite compared with the counterparts with high BPR and low rotation speed and the ones with low BPR and high rotation speed. For the latter two cases, the dissolved Ti in the Cu matrix, caused by the incomplete reaction between Ti and C, significantly reduces

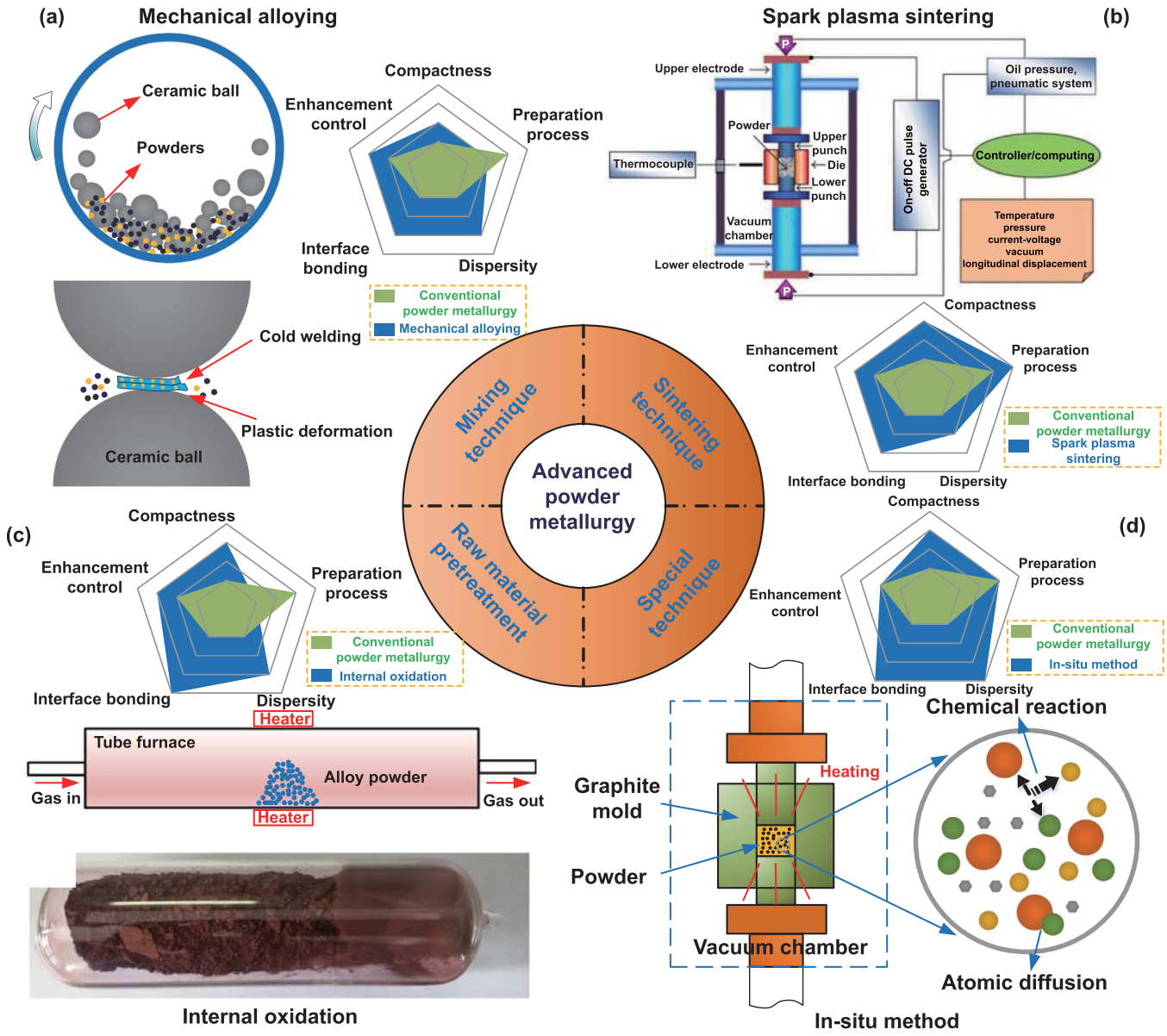

Figure 1. Various preparation techniques and characteristics for advanced powder metallurgy. (a) Mechanical alloying, (b) spark plasma sintering. Reproduced from [29]. CC BY 3.0. (c) Internal oxidation. Reprinted from [30], Copyright (2019), with permission from Elsevier.(d) *In-situ* processing.

the electrical conductivity of the composite but enhances its strength due to solid solution strengthening. However, the agglomeration of fine ceramic particles, especially nanometric particles, is prone to occur during ball milling process. To obtain a uniformly dispersed high-content nanocrystalline Y_2O_3/Cu composite, Huang *et al* [44] adopted a novel approach, namely multi-step ball milling and reduction process, to prepare Y_2O_3/Cu composites. The designed powder mixtures of CuO and Y_2O_3 particles were subjected to milling, reduction, secondary milling and annealing processes. This method can disperse the high content of Y_2O_3 uniformly in the Cu matrix and refining the crystallite size of copper. The yield strength and fracture strain of the Y_2O_3/Cu composite reach 655 MPa and 33.4%, respectively, indicating an effective combination of high strength and large ductility. Meanwhile, the electrical conductivity remains 53.8% IACS (International Annealed Copper Standard). Mechanical alloying has become an important technology to prepare ultrafine-grained and nanoparticle reinforced Cu matrix composites. Note that, in the preparation of Cu matrix composites by mechanical alloying, although long-time ball milling can refine the grains of the composites, it significantly reduces the preparation efficiency. Moreover, impurities are prone to be introduced into the matrix to affect the properties of the composites, especially the conductivity.

2.2. *Sintering technique*

In conventional powder metallurgy processes, a range of thermal diffusion sintering techniques, including pressureless

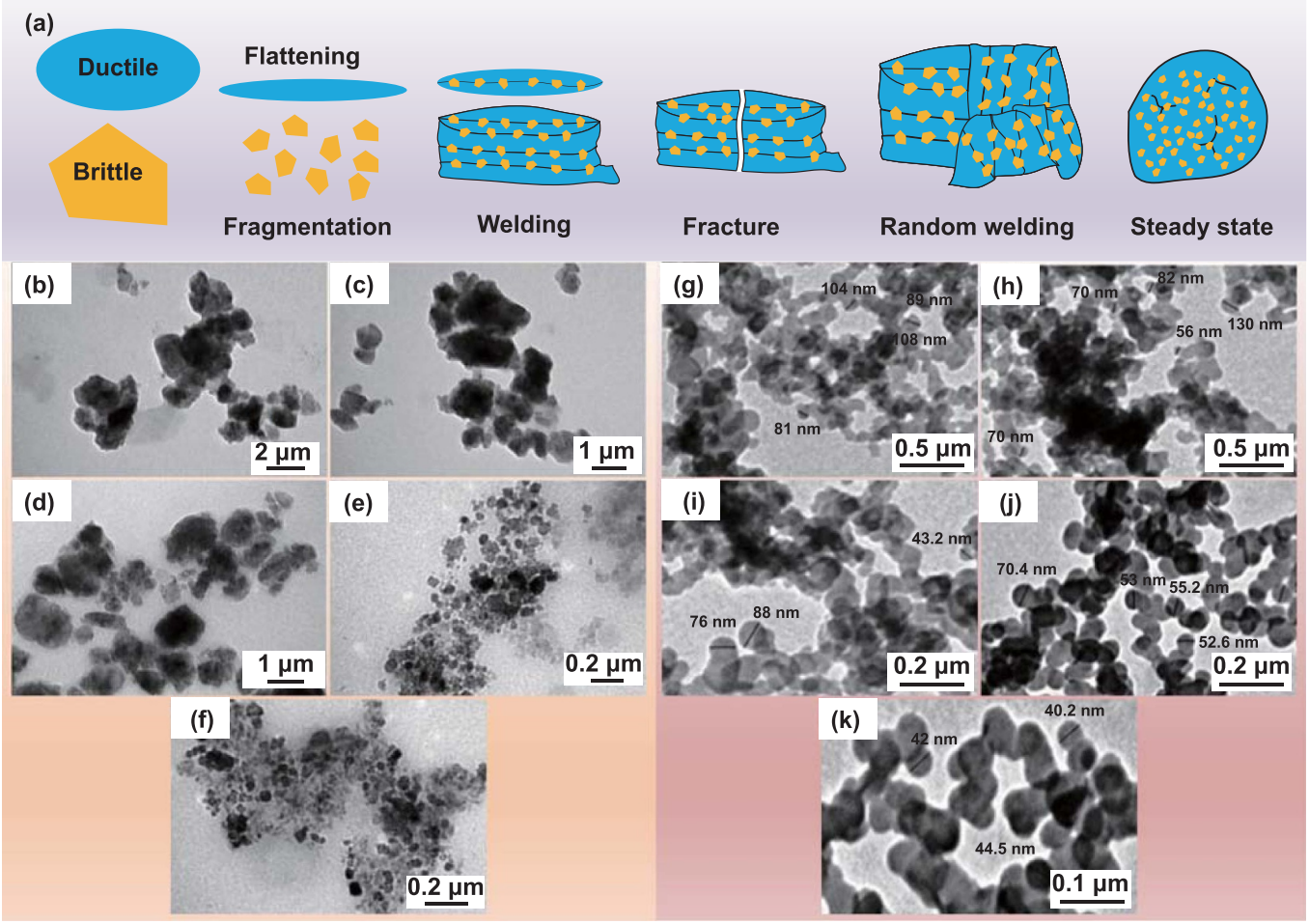

Figure 2. Mechanical alloying process and powder characteristics under different mixing parameters. (a) Various stage of the ductile and brittle powders in the MA process. Reprinted from [38], Copyright (2003), with permission from Elsevier. Transmission electron microscopy (TEM) images of 20 wt.% Al_2O_3/Cu composites after different milling time: (b) 1 h, (c) 5 h, (d) 10 h, (e) 15 h, and (f) 20 h. Reprinted from [39], Copyright (2013), with permission from Elsevier. TEM images of ZrO_2-Cu powders milling for 25 h with different ceramic contents: (g) Cu, (h) 3 wt.% ZrO_2, (i) 6 wt.% ZrO_2, (j) 9 wt.% ZrO_2, (k) 12 wt.% ZrO_2. Reprinted from [40], Copyright (2017), with permission from Elsevier.

sintering, hot press sintering, hot isostatic sintering, etc, are often used to achieve powder consolidation [45, 46]. These thermal diffusion sintering techniques utilize a heat generator around the sample to heat samples, which inevitably prolongs the sintering time and increases energy loss due to thermal diffusion process. In comparison, spark plasma sintering (SPS), a relatively new powder metallurgy sintering technique, can prepare high-performance composite at lower sintering temperature and in shorter sintering time, compared to conventional thermal diffusion sintering methods. In the SPS process, a pulse current is directly applied between the powders for heating and sintering, as illustrated in figures 3(a) and (b). It is widely accepted that the high pulse current applied on the electrode would discharge plasma in the gap between powders, which can effectively eliminate the adsorbed gas and impurities on the surface of powders and destroy the oxide film on powder surface, thereby enhancing the thermal dissemination capability of sintered powder materials [47–50]. To reveal the SPS mechanism, Zhang *et al* [51] demonstrated the existence of spark discharge through direct observations and microstructural analyses. High-temperature spark is formed in the gaps instantly owing to the electrical discharge effect between powders when the switched direct current pulse is energized. Besides, the high heating rate and plastic deformation in the SPS process promote the densification of the sintered materials, thereby significantly improving the sintering efficiency and limiting grain growth.

In general, owing to its unique heating process, SPS-produced samples always exhibit better comprehensive properties compared to the counterparts prepared by conventional sintering process. Naghikhani *et al* [52] compared the effects of pressureless sintering and SPS on the microstructure of WC/brass composites. As shown in figures 3(c)–(f), the composites fabricated by SPS display much more homogenous dispersion of WC particles compared with the pressureless sintered composites. Furthermore, apparent porosities can be observed in the WC-rich region of the pressureless sintered composites. Their results illustrated that the composites sintered by SPS have a density of 92%–97%, which is significantly higher than that of the pressureless sintered ones

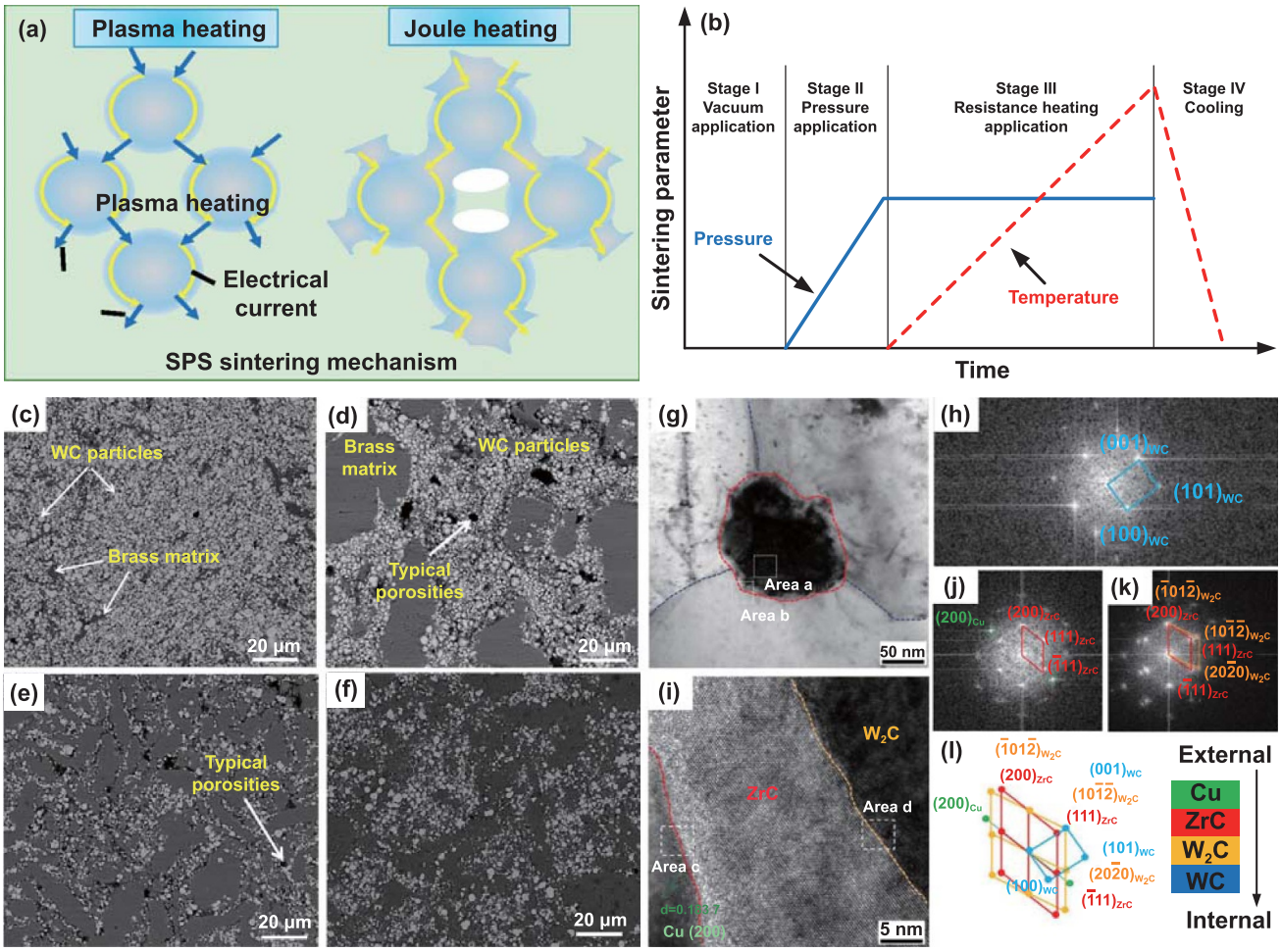

Figure 3. SPS mechanism and resulting microstructure of Cu matrix composites. (a) Schematic of SPS mechanism and (b) SPS stages. Reproduced from [50]. CC BY 4.0. Field emission scanning electron microscopy (FESEM) microstructure of the sintered samples: (c) 30 wt.%WC/Cu-SPSed, (d) 30 wt.%WC/Cu-pressureless sintered, (e) 70 wt.%WC/Cu-pressureless sintered, (f) 70 wt.%WC/Cu-SPSed. Reprinted by permission from Springer Nature Customer Service Centre GmbH: Springer, Metals and Materials International [52], Copyright (2021). (g) TEM image of WC particle in WC/CuCrZr composite; (h) Fast fourier transform (FFT) image of area a in (g); (i) high-resolution TEM (HRTEM) image of the area b in (g); (j) FFT image of area c in (i); (k) FFT image of area d in (i); (l) core–shell particle structure at the interface. Reprinted from [53], Copyright (2022), with permission from Elsevier.

(65%–78%). As such, the SPS-produced composites show about five times higher hardness and higher wear resistance than the pressureless sintered ones. It is well known that different densification mechanisms (e.g. plasticity and creep flow) could directly affect the compactness of powder compacts in the sintering process [29, 54, 55]. During SPS, Joule heating is formed by the conduction of electric current through metals, which results in local vaporization and powder cleaning. This greatly improves the consolidation rate of the SPS process compared to the conventional sintering process. Additionally, the surface of powders can be decontaminated and activated when using pulsed direct current. The heating by the Joule effect leads to a rapid temperature rise, increased mass transfer and material transfer at the macron and micron scales. Therefore, the SPS-fabricated samples exhibit much higher compactness, hardness, strength and wear resistance than the pressureless sintered counterparts. Venkatesh and Deoghare [56] studied the effects of conventional sintering and SPS techniques on the sintering mechanism and mechanical properties of ceramic reinforced metal matrix composites. Compared with the conventional sintered composites, the SPS-fabricated composites exhibit 13.3% higher tensile strength and 11.7% higher compressive strength. Similar scenario was reported in literature, e.g. [57].

For composites and alloys, undesirable microstructural coarsening would decline their mechanical properties due to the high temperature and long conventional sintering time. Furthermore, due to the radial expansion rate exceeding the grain settling and rearrangement rate, cracks tend to develop at grain boundaries in the conventional sintered samples. The SPS technique can effectively solve this problem and improve the mechanical properties [58]. Refined grains could be obtained by SPS owing to the shorter sintering time and lower sintering temperature in the process, which is beneficial

to improve the sintering properties and comprehensive properties of the Cu matrix composites [59–61]. Numerous studies [62–65] have confirmed that the SPS-fabricated sample display significantly smaller mean grain sizes compared with the conventional sintered samples. Moreover, the number of cracks in the samples sintered by SPS is also greatly reduced due to its special heating method.

In addition to the advantages in grain refinement and enhanced densification of Cu matrix composites manufactured by SPS, the higher heat resistance between heterogeneous particles would facilitate interfacial reactions therefore better interfacial bonding. This is also a key factor in the development of Cu matrix composites with enhanced strength-ductility synergy and superior electrical and thermal conductivity. Chmielewski *et al* [66] respectively prepared SiC/Cu composites by hot pressing and SPS. The composites sintered by hot pressing exhibit visible pore aggregation and structural disruption area reaching several microns at interfaces. By contrast, the composites prepared by SPS show better interfacial bonding, resulting in 10% increase in the relative density and 20% increase in the thermal conductivity compared to the composites prepared by hot pressing. As shown in figures 3(g)–(l), the 3 wt.% WC containing CuCrZr composites prepared by mechanical alloying and SPS also display good interfacial bonding [53]. The ZrC and W_2C layers are formed at the interfaces between the CuCrZr alloy and WC particles. Notably, the ZrC layer with 20 nm thick is distributed on the surface of ceramic particles and a W_2C layer is formed inside. According to the orientation relationship of each phase, the ZrC–W_2C–WC core–shell structure transforms the incoherent interface between the WC particles and the Cu matrix into a coherent/semi-coherent interface, which effectively enhances the interfacial bonding between the WC particles and the Cu matrix. For the SPS technique, severe interfacial reaction takes place between the reinforcement and the metal matrix, while such interfacial reactions are very slight and apparent sintering pores are observed in the conventional sintering process [67]. Therefore, the ceramics reinforced Cu composites fabricated by SPS are more compact, with fine grains and high interfacial bonding, resulting in significantly enhanced comprehensive properties of the composites. In short, compared with the conventional thermal diffusion sintering method, SPS has the advantages of fast heating rate, controllable microstructure, energy saving and environmental protection. The prepared composites are more compact and have finer grains and improved interfacial bonding between the ceramic phase and the matrix. However, SPS has difficulty in preparing large-sized products, which is not conducive to industrialization. The formation process of plasma during the powder consolidation and its effect on performance of composites still need to be further explored.

2.3. Raw material pretreatment technique

In order to further improve the interfacial bonding between ceramic particles and the copper substrate, the raw powders used are pretreated by many techniques, such as electroplating, chemical plating, internal oxidation, and so on [68, 69]. Among them, the internal oxidation method is widely adapted owing to its special ability to spontaneously generate oxide particles. In the internal oxidation method, oxygen is dissolved into the alloy powders and diffused in the its constituent phases, and then more active elements in the constituent phases react with oxygen to form uniformly dispersed oxide particles. In this preparation process, the alloy powders are first oxidized and the subsequent treatment is similar to that in conventional powder metallurgy method [70, 71]. Considerable endeavors have been made on the study of Al_2O_3 dispersion strengthened Cu matrix composites. This process could effectively improve the wettability of Al_2O_3–Cu interface and the strengthening ability of hard particles [72–74]. Therefore, uniformly distributed and thermally stable fine oxides are formed in the Cu matrix, and various strengthening mechanisms, such as dispersion strengthening and dislocation strengthening, could fully exert to improve the comprehensive properties of the composites, especially their high-temperature mechanical properties [75].

During the preparation of Al_2O_3/Cu composite, the Cu–Al alloy powders were first melted, then the melt were mixed with the oxidant, and internally oxidized at a certain temperature and atmosphere. Finally, the samples were prepared by the consolidation process. In general, fine Al_2O_3 particles are uniformly dispersed in the Cu matrix, while a small number of coarse particles are distributed on the grain boundaries. The strengthening mechanism at room temperature is mainly determined by the Hall–Petch relation, and the strong pinning effect of Al_2O_3 particles on grain boundaries and sub-grain boundaries is responsible for the high-temperature strengthening. On this basis, Zhao *et al* [76] prepared the Al_2O_3 dispersion strengthened Cu composite by a combination of internal oxidation and mechanical alloying. Their results demonstrated that this compound process could enable the aluminum to be oxidized completely in 10–20 h, which is much faster that only by mechanical alloying (exceeding 40 h). The uniform distribution of Al_2O_3 particles and the refined reinforcing particle for this compound process are conducive to obtain better comprehensive properties. However, in the process of atomized Cu-Al alloy powders and high-energy mechanical milling, the impurities in the powders could sharply reduce the properties of the Al_2O_3/Cu composites. Li *et al* [30] adopted a novel method to fabricate ultrafine-grained Al_2O_3/Cu bulk composites, as shown in figure 4(a). Firstly, the Al–Cu alloy powders were dealloyed to prepare nanocrystalline powders; then the dealloyed powders were heat-treated by two different methods; the powders were finally consolidated by powder compact extrusion. The locations of the Al_2O_3 nanoparticles in relation to the heat treatment route result in formation of two kinds of microstructures. The Al_2O_3 nanoparticles of the R1-treated composite are mainly distributed at grain boundaries, and the Al_2O_3 nanoparticles of the R2-treated composite are mainly distributed within grains, as illustrated in figure 4. As a result, the intragranular Al_2O_3 nanoparticles are more beneficial to realize a good strength-ductility synergy and high electrical conductivity.

After internal oxidation process, partial sintering occurs between the powders due to local high temperatures caused by

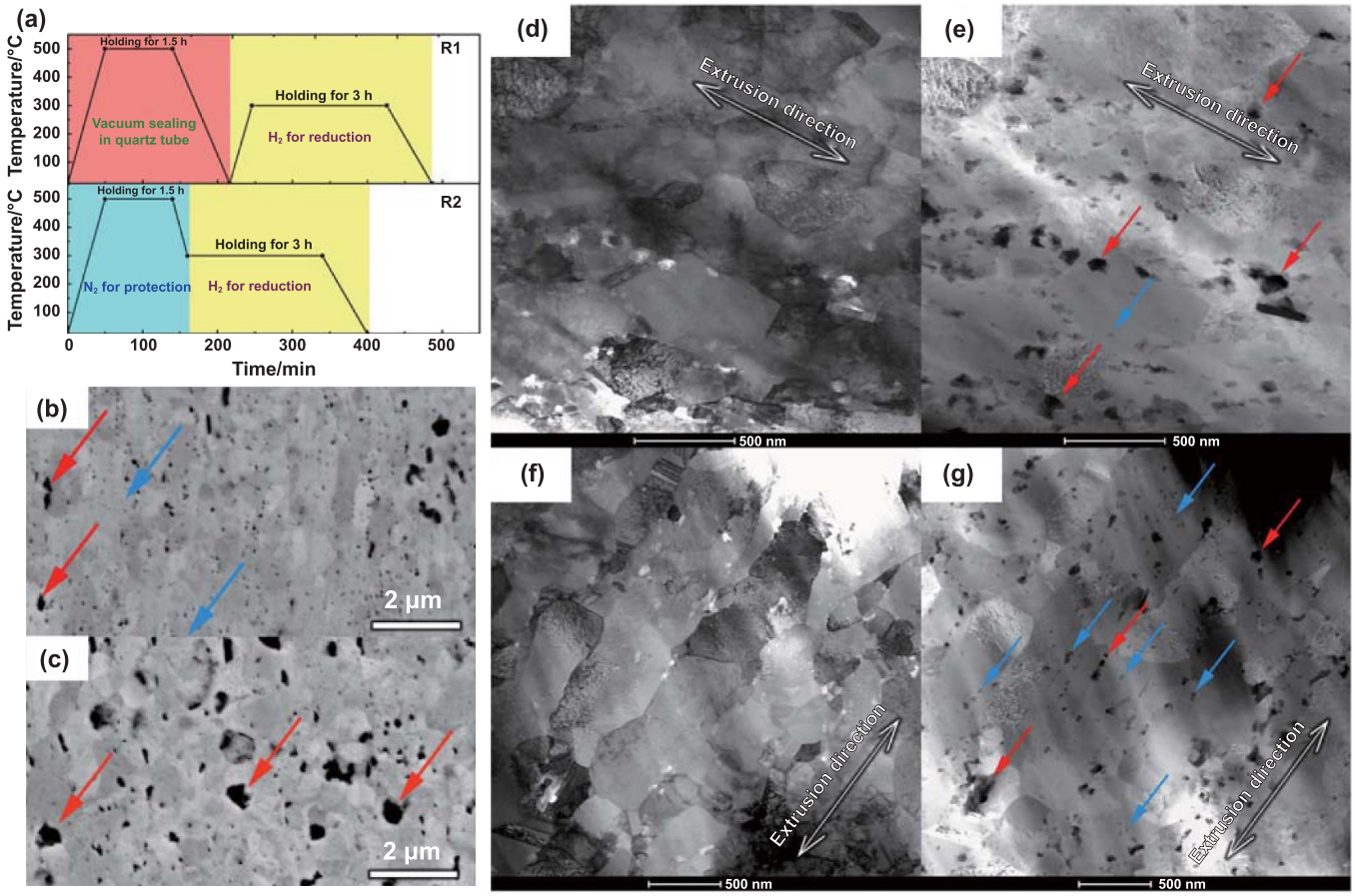

Figure 4. Microstructural characteristics of Al_2O_3/Cu composites fabricated by a novel internal oxidation method. (a) Schematic diagram of temperature-time for two heat treatment routes, R1 and R2, respectively. SEM images of (b) R1-treated sample and (c) R2-treated sample. Scanning transmission electron microscopy-Bright field (STEM-BF) images ((d) and (f)) and STEM-HAADF (High-angle annular dark field) images ((e) and (g)) of (d) and (e) R1-treated samples and (f) and (g) R2-treated samples. The intergranular Al_2O_3 and intragranular Al_2O_3 particles are indicated by red and blue arrows, respectively. Reprinted from [30], Copyright (2019), with permission from Elsevier.

the exothermic internal oxidation reaction, so the quantity of fine particles is significantly reduced. Meanwhile, the Al_2O_3 particles are easily coarsened and agglomerated in the composite and cannot achieve the desired strengthening effect. In order to reveal the reasons for this phenomenon, a combining study between powder metallurgy and Rheins-pack method was conducted [77]. The experimental results suggested that the particles tend to preferentially aggregate at grain boundaries, and the increase in both diffusion distance and Al content would coarsen the particles. Even worse, coarsening and agglomeration of Al_2O_3 particles are accelerated due to the presence of water vapor during the internal oxidation process, and coarse and agglomerated particles are generated on the powder surface during water atomization. Ti doping was also found to effectively refine the size and modify the intergranular and intragranular Al_2O_3 particles [77, 78]. Similar work was also carried out on the effect of Ag addition on the morphology and size distribution of Al_2O_3/Cu composites [79]. The addition of Ag promotes the diffusion of oxygen atoms in the Cu matrix and the internal oxidation process. This is because the Ag doping provides more 'tunnels', such as grain boundaries and lattice defects, for oxygen atoms to diffuse in the Cu matrix, which allows oxygen atoms to diffuse through the dense Al_2O_3 layer to the reaction front for a continuous internal oxidation process with Al. The particle size of Al_2O_3 particles decreases from ~63 nm to ~37 nm as increasing the Ag content, and numerous triangular Al_2O_3 precipitates are observed in the Ag-doped Al_2O_3/Cu composites. Increasing the Ag amount can enhance the electrical conductivity and mechanical strength of the Al_2O_3/Cu–Ag composite. When the Ag/Al atomic ratio is ~1:4, the composite exhibits the optimal electrical of 85.9% IACS and hardness of 162 HV.

Recently, different consolidation methods of internal oxide powders have also attracted extensive attention. Three consolidation methods, i.e. high-speed compaction, hot pressing and hot extrusion, were used to compare their effects on the microstructure and properties of internal oxide Al_2O_3 dispersion strengthened Cu matrix composites [74]. The composites prepared by hot pressing display the coarsest grains while the counterparts prepared by hot extrusion have the finest grains. This is attributed to the repeated stretching and pulling of the powder particles during hot extrusion, which eliminates residual pores and refines the grains. In contrast, grain growth is not restricted in the hot-pressing process. The composites prepared by high-speed compaction method exhibit the lowest relative density of 98.3% (versus 99.5% for the ones by

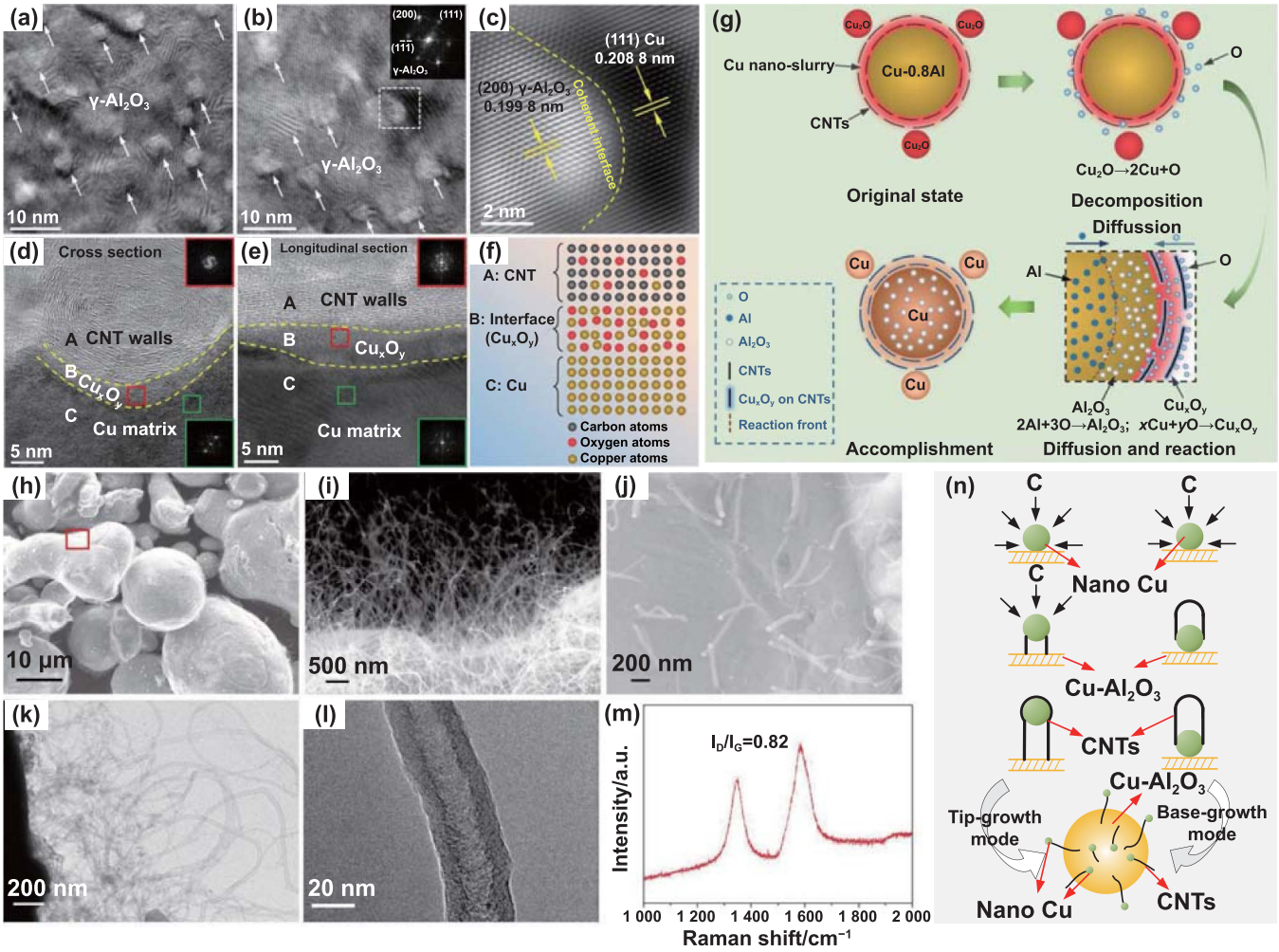

Figure 5. HRTEM images of the interfacial characteristics for Al_2O_3–Cu and CNTs–Cu. (a) Distribution image of Al_2O_3 and FFT inset. (b) Characterization of the interface between Al_2O_3 and Cu matrix. (c) Interplanar space measurement between Al_2O_3 and Cu matrix. (d) Cross-sectional image of CNT/Cu interface. (e) Longitudinal sectional image of CNT/Cu interface. (f) Schematical diagram of CNTs/Cu interface. (g) Schematic diagram of oxygen diffusion and *in-situ* solid-reaction for Cu–Al_2O_3-CNTs. Reprinted from [80], Copyright (2022), with permission from Elsevier. SEM images (h)–(j) of the CNTs/Al_2O_3/Cu composite powders, TEM images (k), (l) and Raman spectra (m) of CNTs. (n) Schematic diagram of growth mechanism of CNTs on the Al_2O_3/Cu powder. Reprinted from [81], Copyright (2019), with permission from Elsevier.

hot pressing and 100% for the counterparts by hot extrusion) owing to the small amount of air entrained in the composites during the rapid compaction process. This leads to the minimum electrical conductivity of 81% IACS (versus 86% IACS for the ones by hot pressing and 87% IACS for the counterparts by hot extrusion). However, the higher strength could be obtained by the composites prepared by high-speed compaction owing to severe plastic deformation and dislocation formation. Furthermore, the composites prepared by high-speed compaction demonstrate higher softening temperature and high-temperature serviceability.

In addition to the manipulation of the particles in the composites, good interfacial bonding between ceramic particles and Cu matrix is also required for obtaining a composite with excellent properties. The fully coherent interface between internal oxidized Al_2O_3 and Cu matrix is conducive to accumulating high-density dislocations in the interior of grains and hindering dislocation motion, thereby significantly enhancing the strength-ductility synergy of Cu matrix composites. Oxidation-induced nano-Al_2O_3 particles and interface-optimized carbon nanotubes (CNTs) could significantly enhance the strength of Cu matrix composites and preserve their plasticity. Based on this strategy, Long *et al* [80] developed an internal oxidation method for preparing high-performance Al_2O_3/Cu matrix composites doping with CNTs. As shown in figures 5(a)–(g), coherent Al_2O_3 nanoparticles are formed in CNTs and amorphous copper oxide (Cu_xO_y) is formed between CNTs and Cu, due to the diffusion of oxygen atoms and *in-situ* reactions resulting from the thermodynamic driving forces during internal oxidation process. The combined strengthening role of Al_2O_3 nanoparticles and interface-optimized CNTs enables the composite to obtain high mechanical properties (tensile strength of 510 MPa and plasticity of 20.2%). The Al_2O_3 nanoparticles and CNTs render the

composite high strength because of Orowan strengthening and high-efficiency load transfer strengthening. Meanwhile, the synergistic effect of the internal dislocation stacking of Al_2O_3 nanoparticles and the enhanced crack resistance by optimized CNTs interfacial bonding collectively contributes to the tensile ductility.

The CNTs/Al_2O_3/Cu composites can also be produced by *in-situ* chemical vapor deposition (CVD) [81]. The Al_2O_3/Cu powders were obtained by the internal oxidation method and the CNTs were compounded *in-situ* on the surface of powders by CVD, as illustrated in figures 5(h)–(n). The CNTs are distributed individually in the matrix and they do not agglomerate on the powder surface. Besides, the wall surfaces of CNTs are clean with no amorphous carbon, and the diameter of the CNTs tubes is uniform over the whole length at about 20 nm. The presence of Al_2O_3 on the CNTs surface promotes to form Cu nanoparticles, thereby facilitating the growth of CNTs. The CNTs with high surface cleanness and high degree of graphitization are evenly distributed on the surface of composite powders and are well bound with the matrix. Subsequently, the SPS technique was employed to sinter CNTs/Al_2O_3/Cu bulk composites [82]. In bulk composites, the CNTs that are well bound with the Cu matrix and Al_2O_3 particles play a synergistic role in enhancing the mechanical and electrical properties. Since Al_2O_3 and CNTs are distributed at grain boundaries, the Zener pinning effect is responsible for the inhibition of grain growth in the Cu matrix.

In brief, the internal oxidation method can be used to prepare uniformly distributed and thermally stable fine oxides in Cu matrix composites to obtain excellent comprehensive properties, especially high-temperature mechanical properties. Besides, doping CNTs in the composite by internal oxidation can further improve the interfacial bonding and play a synergistic role in enhancing the mechanical and electrical properties. Nevertheless, in additional to its complicated process and high cost, the control of oxygen content is the challenge in preparing Cu matrix composites by this method. This is also a key problem to realize large-scale and industrialized production of Cu matrix composites.

2.4. Special technique

The *in-situ* synthesis method is a novel preparation technique developed in recent years for fabricating Cu matrix composites in which a series of thermo-mechanical treatments or chemical reactions take place under certain conditions to form one or more reinforcing phases inside the matrix with aim to improve the performance of composites [83–86]. However, most of the reinforcements are prone to aggregate and coalesce at the grain boundaries of the Cu matrix and to form semi-coherent or incoherent interfaces with the Cu matrix because they have radically different physical and chemical properties from the Cu matrix [87]. On this basis, *in-situ* synthesis method could perfectly solve the disadvantages that are demonstrated in the composites fabricated by *ex-situ* preparation methods (addition of existing ceramic phases), such as poor interfacial wettability and weak interfacial bonding between the reinforcing phases and the Cu matrix. As such, the *in-situ* Cu matrix composites generally demonstrate good thermodynamic stability with refined and homogeneously distributed reinforcements in Cu matrix [88–91].

In the *in-situ* prepared Cu matrix composites, ceramic or intermetallics including oxides, carbides, borides, etc, are *in-situ* formed in the Cu matrix. Among the *in-situ* generated reinforcements, some rare earth oxides with superior thermodynamic stability are attractive as dispersions in composites. Furthermore, these rare earth elements with larger atomic radii exhibit low solubility and diffusivity in the Cu matrix, which would improve the microstructure stability and prevent grain coarsening [92, 93]. However, this also limits their ability to prepare Cu matrix composites by internal oxidation methods. To obtain uniformly distributed oxides in the Cu matrix, Zhou *et al* [94] used Cu–Y alloy to prepare Y_2O_3/Cu composites by *in-situ* synthesis method at the liquidus temperature. Microstructure transformation takes place during the solidification of the molten Cu–Y alloy, accompanied by an *in-situ* formation of Y_2O_3 particles. On the one hand, yttrium reacts with oxygen (which is diffused into the solution) to form Y_2O_3 particles. Meanwhile, the yttrium content in the regions around the particles is locally reduced and a supercooled zone is formed around the Y_2O_3 particles. On the other hand, Y_2O_3 particles can act as a nucleation agent to further promote solidification. This promotes the isothermal solidification of the Cu–Y melt, which results in the formation of an equiaxed microstructure. As a result, the nano-sized rare earth oxides with an average grain size of 5 nm and interspacing of 20 nm are evenly distributed in the matrix and are coherent with the Cu matrix. Under the joint strengthening effect of Orowan and shearing mechanism, the prepared Y_2O_3/Cu composite exhibits significantly higher ultimate tensile strength than the pure Cu.

Compared to the oxide enhancements, *in-situ* synthesized carbides and borides are easier to generate in Cu melts and to avoid the oxidation of the Cu matrix. Furthermore, most carbides and borides, such as TiC, NbC, TiB_2, ZrB_2, and so on, demonstrate better interfacial bonding and comprehensive properties. Generally, these *in-situ* enhancements are formed by the chemical reaction of Mc (=Zr, Ti) and Nm (=C, B, BN, B_4C) in the Cu–Mc–Nm systems. For instance, *in-situ* TiB_2/Cu composites were generated through exothermic dispersion synthesis in the Cu–Ti–B system [95]. As shown in figure 6, intermediate phase Cu_4Ti is first formed by the reaction of Cu and Ti, and then Cu_4Ti reacts with B to form uniformly distributed ultrafine-grained TiB_2 particles as the reinforcement. The reaction process in this system can be described as: $Cu + Ti + B \rightarrow Cu_4Ti + B \rightarrow Cu + TiB_2$. Meanwhile, the ultrafine TiB_2 particles are uniformly distributed in the Cu matrix, which greatly enhances the mechanical performance of the composites. On this basis, the Cu matrix can be a catalyst for *in-situ* reaction. The Cu matrix first reacts with the reactant Mc (=Zr, Ti) to form the intermetallic compound and then reacts with the reactant Nm (=C, B, BN, B_4C) to form the ceramic phase. This process can lower the temperature threshold of the reaction and allow the *in-situ* reactions below the liquidus of Cu matrix, which facilitates grain refinement and enhances the dispersion of ceramic particles.

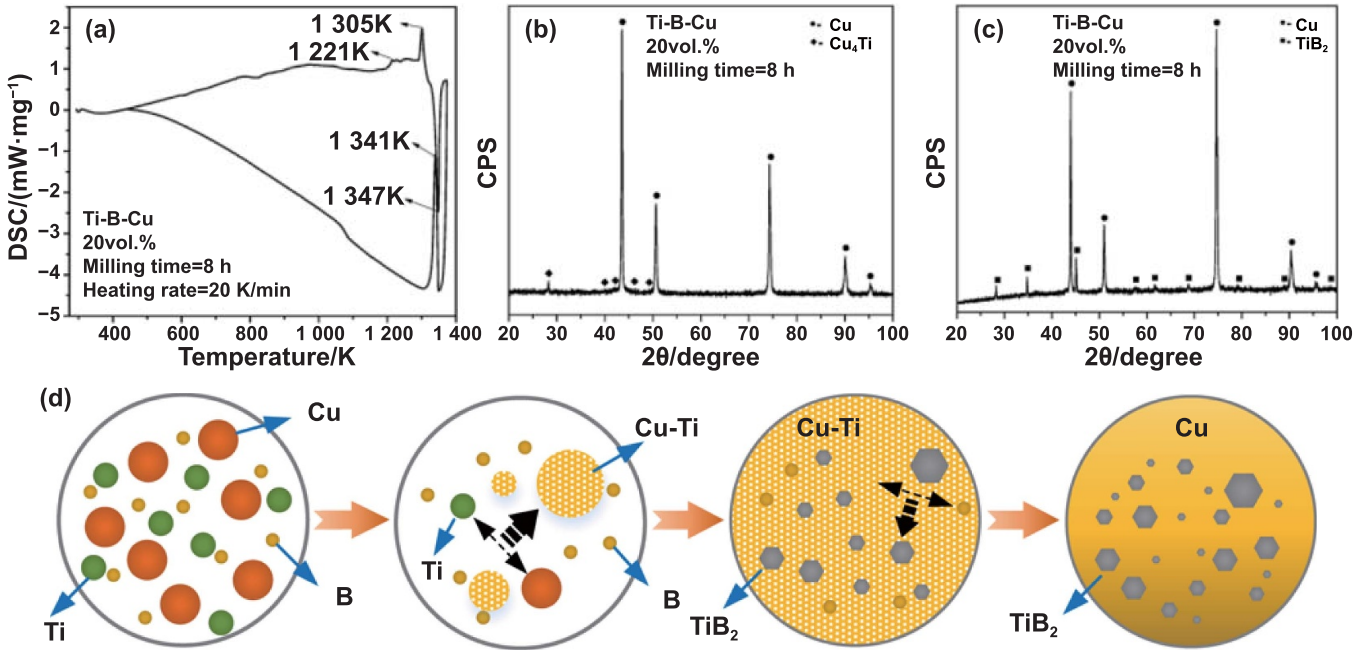

Figure 6. The differential scanning calorimetry (DSC) curve and x-ray diffraction (XRD) patterns of the reacted TiB_2/Cu composites. (a) DSC curves; XRD patterns of the sample heated to (b) 1233 K and (c) 1373 K. (d) Schematic diagrams of the microstructure formation of the TiB_2 particles. Reprinted from [95], Copyright (2017), with permission from Elsevier.

However, during the preparation process, not all the added reactants could be fully reacted. The added Nm (=C, B, BN, B_4C) reactants tend to react incompletely with the solute Mc (=Zr, Ti) reactants to form ceramic phase owing to their poor wettability and limited solubility in Cu melts. The residual reactants would dissolve into the Cu matrix and induce deformation of the surrounding lattice, thus scattering electrons and significantly affecting the conductivity of the composite. Ding *et al* [96] found that only around 70% of graphite has reacted with soluble Ti to form TiC. Thus, element B was added into the composite to dissipate the remaining Ti by forming TiB_2. Their results showed that the introduction of B improves the distribution homogeneity of the reinforcing particles, thereby enhancing the hardness and electrical conductivity of the Cu matrix composites. Guo *et al* [97] prepared the molybdenum carbide coated graphene (GNP) nanosheets (Mo_2C@GNPs) through a combination of impregnation reduction and *in-situ* reaction. As shown in figures 7(a)–(g), Mo_2C is uniformly dispersed both at the interfaces between GNPs and the Cu matrix and in the Cu matrix adjacent to GNPs. This demonstrates that Mo_2C not only modifies the interface between the reinforcements and the matrix but also acts as a reinforcement phase dispersed around the GNPs. As a result, the Mo_2C@GNPs reinforced Cu matrix composite demonstrates yield strength reaching 303 MPa, which is 72% and 23% higher than the corresponding ones for pure Cu (176 MPa) and GNPs/Cu composite (247 MPa), respectively, and electrical conductivity exceeding 90% IACS.

In the process of *in-situ* synthesis, the type, physicochemical properties and adaptability of reactants directly determine the reinforcing effect of the products. Zhang *et al* [98] fabricated *in-situ* TiC/Cu composites by combustion synthesis and hot pressing in the Cu–Ti–CNTs system. By controlling the mixing mode of CNTs, TiC particles with different sizes and morphologies were formed in the composites and exhibited different reinforcing effects. In addition to the pretreatment of the reactants, using different sources of reactants could also greatly affect the *in-situ* synthesis. Previous work [99] intensively investigated the effect of carbon sources (graphite, CNT and graphene) on the phases formation and comprehensive performance of *in-situ* TiC–C/Cu composites in the Cu–Ti–C system. Among the carbon sources, CNTs and graphene can promote to form fine TiC nanoparticles, which greatly enhances the tribological properties of the Cu matrix composites. The previous work from the current team [100] prepared high-volume-fraction TiB_2/Cu and (TiC + TiB_2)/Cu composites in the Cu–Ti–B and Cu–Ti–B_4C systems by the *in-situ* method. As shown in figure 8(a), the reactions are sufficient, and only diffraction peaks of TiB_2, TiC and Cu are detected. The ceramic particles in the Cu matrix are evenly distributed without evident pores and aggregation of particles (figures 8(b) and (c)). Computational simulation results suggested that the nearly spherical ceramic particles could modify the thermal transfer routes and stress–strain response and reduce stress concentration, which further enhances its properties (figures 8(d)–(f)). From the above results, *in-situ* synthesis has become a promising technique for the preparation of Cu matrix composites. This process could effectively solve the challenges of poor interfacial wettability and reduce the pretreatment process of the reinforcing phase, further simplifying the preparation process. However, this method has high requirements on reactants and it can only prepare reinforcements with good reactivity and matrix compatibility. Furthermore, further in-depth understanding is need on

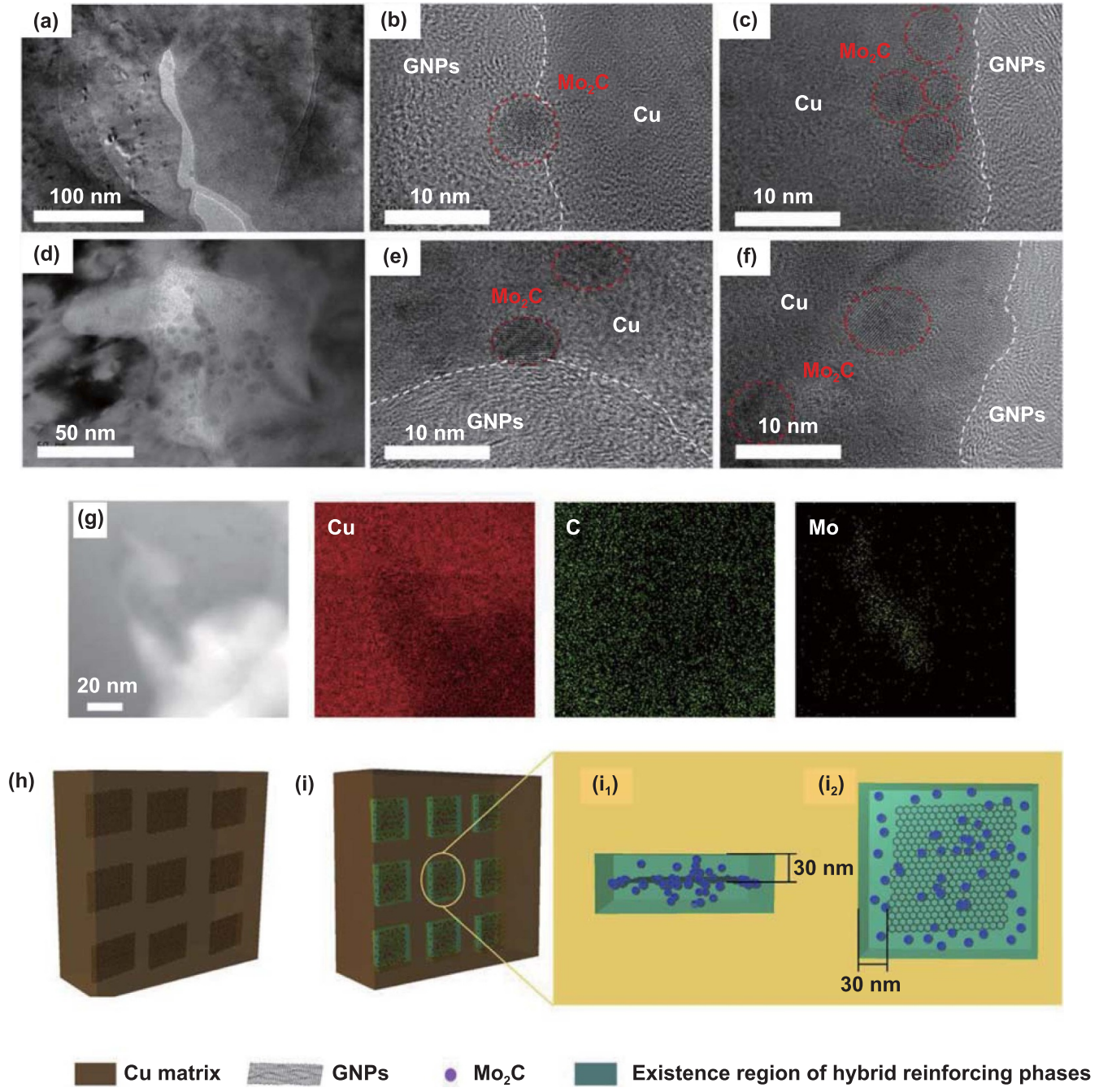

Figure 7. Detailed TEM and HRTEM characterizations of molybdenum carbide distribution in Cu matrix composites. (a), (d) TEM images of Cu-1.6GNPs-0.11Mo_2C; (b), (c), (e), (f) HRTEM images of Cu-1.6GNPs-0.11Mo_2C; (g) STEM and EDS images of Cu-1.6GNPs-0.11Mo_2C. Schematic diagrams of hybrid reinforcing phases distribution of (h) GNPs, (i) GNPs@Mo_2C. Reprinted from [97], Copyright (2019), with permission from Elsevier.

precisely controlling of the content and morphology of the enhanced phase and the *in-situ* reaction process to improve the comprehensive performance of Cu matrix composites.

In conclusion, the Cu matrix composites fabricated by various techniques tend to possess different comprehensive properties [61, 101]. The Cu matrix composites by these advanced preparation processes, including mechanical alloying, spark plasma sintering, internal oxidation and *in-situ* processing, demonstrate better comprehensive properties compared with the counterparts prepared by conventional powder metallurgy process. Table 1 summarizes the advantages and disadvantages of various advanced techniques. Among them, the dispersion of ceramic particles in the Cu matrix and the interfacial bonding between ceramic particles and the Cu matrix are greatly enhanced in the Cu matrix composites prepared by these advanced techniques. Meanwhile, the combination of these processes can further enhance the comprehensive properties of Cu matrix composites.

Figure 9 summarizes the comprehensive performance of Cu matrix composites prepared by various processes reported

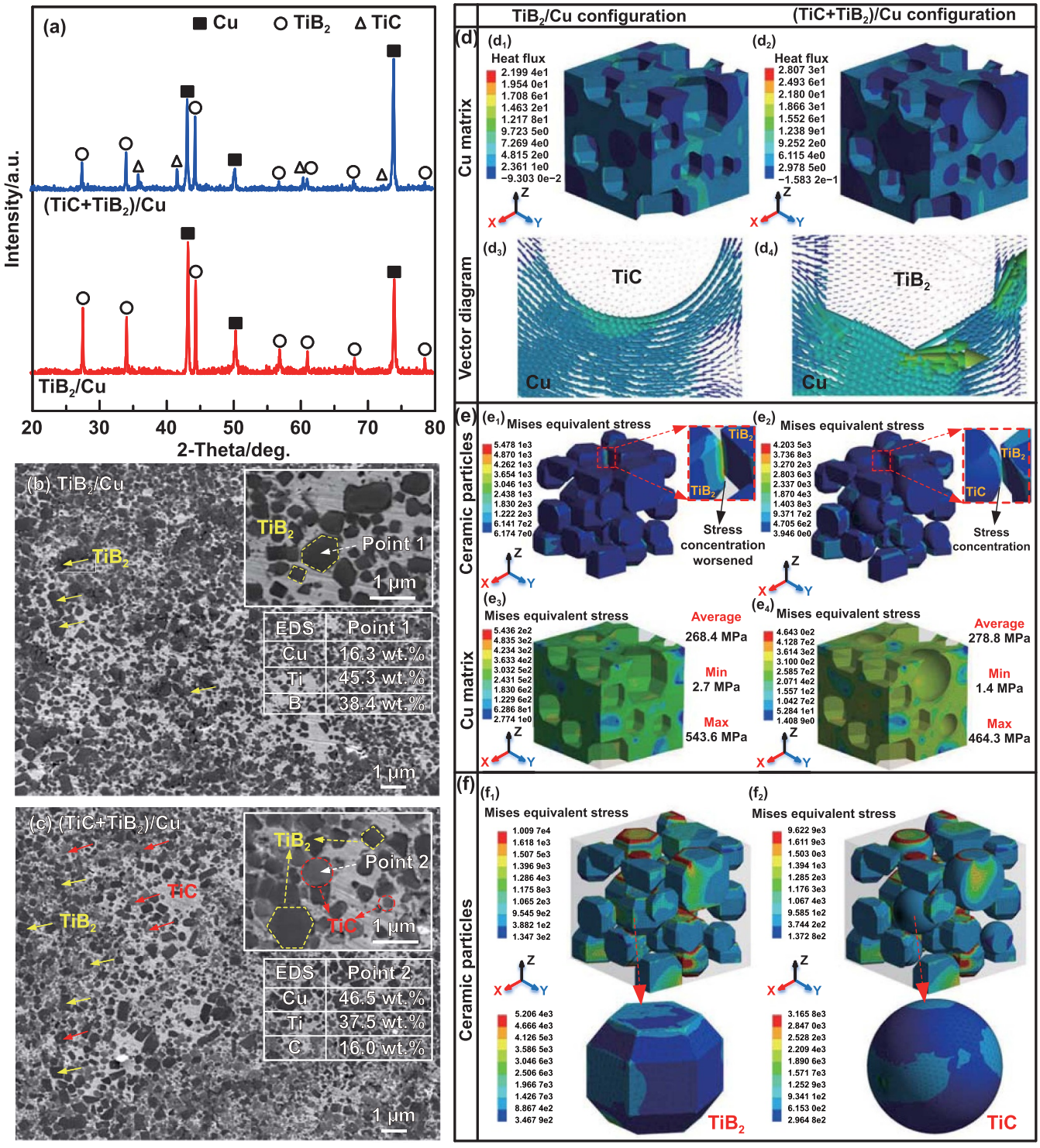

Figure 8. Microstructure and finite element modeling (FEM) results of *in-situ* TiB_2/Cu and (TiC + TiB_2)/Cu composites. (a) XRD spectrums of the *in-situ* TiB_2/Cu and (TiC + TiB_2)/Cu composites. (b), (c) FESEM images for these two composites. (d) Heat flux distribution of (d_1, d_2) Cu matrix for these two composites, and the corresponding (d_3, d_4) interface vector diagrams. (e) Thermal residual stress (MPa) of (e_1, e_2) ceramic particles and (e_3, e_4) Cu matrix for these two composites after cooling. (f) Equivalent stress (MPa) distribution of (f_1, f_2) ceramic particles for these two composites. Reprinted from [100], Copyright (2022), with permission from Elsevier.

in the literature. The representative performance of ceramic reinforced Cu matrix composites prepared by various processes are summarized in table 2. It can be found that the Cu matrix composites prepared by combining multiple advanced techniques tend to exhibit better synergistic strengthening effects in strength-ductility and strength-conductivity. For instance, 1.1Al_2O_3/Cu composites fabricated by internal oxidation followed by hot extrusion demonstrate excellent synergetic enhancement in strength-ductility and in electrical conductivity [73]. Their yield strength and fracture strain are

Table 1. Comparison of the advantages and disadvantages of different advanced techniques.

Preparation technique	Advantages	Disadvantages
Mechanical alloying	Interatomic diffusion; ultrafine-grained and nanoparticle	Low preparation efficiency; easy to introduce impurities
Spark plasma sintering	High preparation efficiency; finer grains and higher interfacial bonding;	Not good for industrialization
Internal oxidation	Coherent interface; improved interfacial wettability; fine oxides	Complicated process and high cost; precise control of oxygen content
In-situ processing	Coherent interface; particle morphology control; further simplification of the preparation process	Specific reactants; incomplete reaction

533 MPa and 25% respectively, and their electrical conductivity is still maintained at 85% IACS. Generally, the Cu matrix composites prepared by combining advanced processing techniques would further increase the relative density (i.e. compactness), refine the grains, and optimize the dislocation distribution of ceramic reinforced Cu matrix composites. This is beneficial for repairing the defects of the specimens during the process of powder metallurgy, thereby enhancing their comprehensive performance. Therefore, further combining the advanced preparation processes along with appropriate processing techniques is the focus of future work.

3. The effects of ceramic particles on the comprehensive properties of Cu matrix composites

The superior electrical conductivity and thermal conductivity of Cu make it an indispensable functional material in the application fields of heat transfer and conductive components. In the application of electrical contact materials, heat transfer and conductive components, such as integrated circuit lead frame and brush, high strength and high conductivity of the materials are indispensable [108–110]. In the new era, to overcome the shortcomings of low strength, low stiffness and poor wear resistance of Cu, numerous studies have been carried out to introduce alloying elements to enhance the strength of Cu by grain refinement strengthening, work hardening and precipitation strengthening [111, 112]. The Cu–Fe–P [113], Cu–Ni–Si [114] and Cu–Cr–Zr [115, 116] alloys are representative Cu alloys with high strength and high conductivity. However, the strength of these alloys decrease dramatically above 400 °C and the tensile strength is even lower than 100 MPa at 600 °C due to the dissolution or coarsening of the precipitated phases [117, 118]. In contrast, ceramic particles with high specific strength and high-temperature stability as reinforcement can effectively impede the movement of dislocations and migration of grain boundaries, thus significantly enhancing the mechanical properties of Cu matrix composites at both room temperature and high temperatures [119–121]. Unfortunately, the low conductivity of the ceramic phase and the lattice distortion in the Cu matrix caused by the ceramic particles would inevitably reduce the thermal and electrical conductivity of the Cu matrix [122, 123]. However, the effect of ceramic particles on conductivity is little compared to the enormous scattering effect of solute atoms on free electrons in Cu alloys [112, 124]. For example, the incorporation of 0.89 at.% solute atomic Cr results in a 170% increase in electrical resistivity. Zhang *et al* [125] also demonstrated that the thermal conductivity of matrix doped with alloying elements is much lower than that of the Cu matrix composites with the addition of ceramic particles. In addition, to minimize the weakening effect of conductivity by ceramics, low content (<5 wt.%) of ceramic particles was proposed to modify the mechanical properties of Cu matrix composites on the premise of ensuring their thermal and electrical conductivity. Qin *et al* [126] prepared (1, 3, 5 wt.%) Y_2O_3/Cu composites by solid–liquid doping, calcination reduction and SPS. The Y_2O_3 particles are primarily dispersed at the Cu grain boundaries, and its distribution changes from dispersion to aggregation as increasing the Y_2O_3 content. Besides, the introduction of Y_2O_3 into the Cu matrix can effectively refine the matrix grains. Due to the dispersion strengthening effect of Y_2O_3, the strength and hardness of the composites are greatly enhanced, and the electrical conductivity is remained at 95% IACS. Therefore, ceramic reinforced Cu matrix composites with low particle content are highly competitive materials in achieving synergistic enhancement of strength and conductivity.

In the application of integrated circuits, the packaging material plays the role of chip protection, chip support, chip heat dissipation, chip insulation and connection between the chip and the external circuit. The research focus on electronic packaging materials shifts from metals, ceramics and plastics to composites [109, 127]. In the electronic packaging material, the material should possess good thermal conductivity, which can conduct the heat generated by the semiconductor chip in time; the CTE of the material should be small to avoid chip damage due to thermal stress when matching with Si or GaAs chips; the material needs to play a certain role in supporting and protecting the chip, thus requiring a certain strength [128, 129]. Although Cu matrix composites exhibit high applicability in electrical packaging owning to their high thermal conductivity, the high CTE and poor mechanical properties of Cu are not sufficient for packaging materials. In order to reduce its CTE, the reinforcing phase with low CTE and density, such as ceramics and diamond, is often compounded with the Cu matrix to obtain the more ideal electrical packaging material. Furthermore, the introduction of ceramic particles could also greatly improve the strength and wear resistance of the Cu matrix composite. In this field, high content of ceramic particles is usually introduced to reduce the CTE of Cu matrix composites and to enhance their mechanical properties. Lu *et al* [107] found that the increase in ceramic content would enhance the mechanical properties of the 40–60 vol.% TiC–TiB_2 reinforced Cu matrix composites.

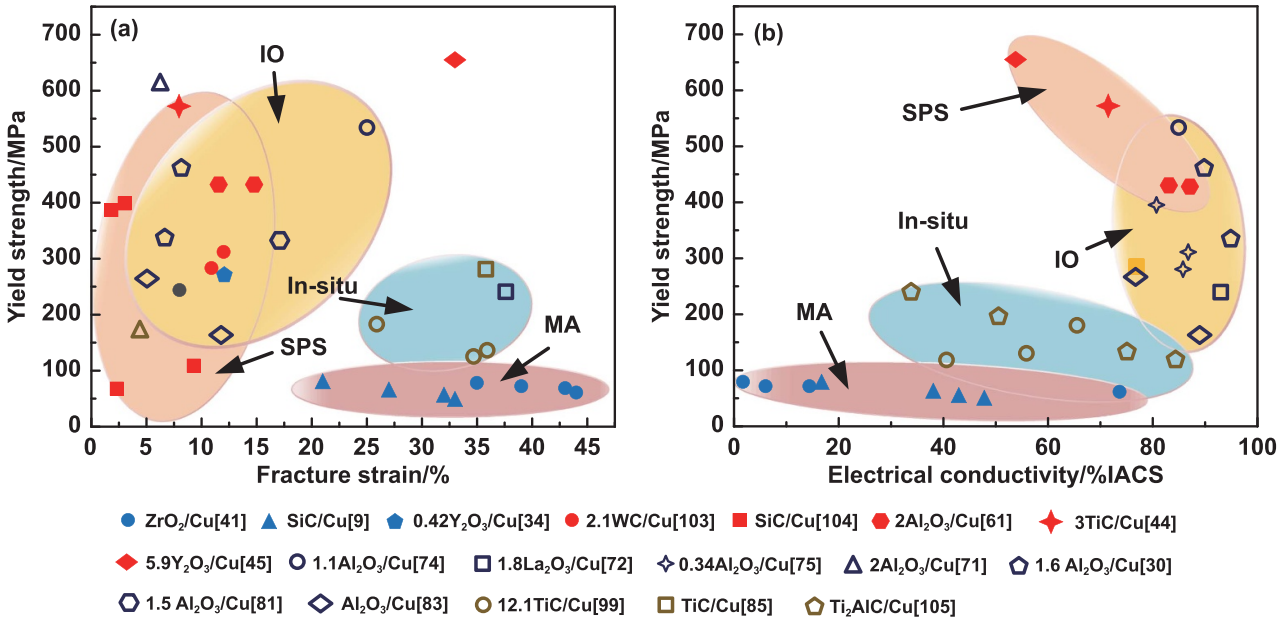

Figure 9. Comparison of the properties in ceramic reinforced Cu matrix composites prepared by different processes. (a) Yield strength versus fracture strain; (b) yield strength versus electrical conductivity.

For the 60 vol.% TiC–TiB_2 containing composite, the ultimate compression strength and hardness reach 1346 MPa and 448 HV, respectively. The wear rate is only one-third that of the pure Cu. When an external load is applied, stress transfers from the 'soft phase' to the 'hard phase', and the reinforcing particles can effectively sustain most of the loads, thereby significantly enhancing the strength of the composite. Previous work from the current team [100] also demonstrated that the Cu matrix composite with high-content ceramic particles have a low CTE (8.5×10^{-6} K^{-1}) and their thermal conductivity reaches 122 W $(m{\cdot}K)^{-1}$ at room temperature.

3.1. Effect of ceramic particles on the mechanical behaviors of Cu matrix composites

As known, ceramic particles can greatly enhance the strength and wear resistance of metal matrix composites. The ceramic particles with high specific elastic modulus effectively increase the Young's modulus and yield strength of the Cu matrix composites. In theory, the Young's modulus of ceramic particles reinforced Cu matrix composites is predicted by the classical Hashin–Shtrikman elasticity theory [130]:

$$E_{\text{HS - Upper}} = \frac{E_p\left[E_p V_p + E_m\left(2 - V_p\right)\right]}{E_m V_p + E_p\left(2 - V_p\right)} \tag{1}$$

$$E_{\text{HS - Lower}} = \frac{E_m\left[E_m\left(1 - V_p\right) + E_p\left(1 + V_p\right)\right]}{E_m\left(1 + V_p\right) + E_p\left(1 - V_p\right)} \tag{2}$$

$$E_{\text{HS}} = \left(E_{\text{HS - Upper}} + E_{\text{HS - Lower}}\right)/2 \tag{3}$$

where V is the volume fraction and E is the Young's modulus. The subscripts c, m, and p denote the composite, matrix, and particle, respectively. $E_{\text{HS - Upper}}$ and $E_{\text{HS - Lower}}$ are the upper limit and the lower limit of Hashin–Shtrikman theory, respectively, and E_{HS} is the Young's modulus of the composite predicted by Hashin–Shtrikman theory.

For Hashin–Shtrikman elasticity theory, only the Young's modulus and content of the matrix and ceramic phases are considered. While the Tsai–Halpin equation takes into account the aspect ratio of ceramic particles, and it is expressed as [131]:

$$E_c = \frac{E_m\left(1 + 2s\tau V_p\right)}{1 - \tau V_p} \tag{4}$$

$$\tau = \frac{E_p/E_m - 1}{E_p/E_m + 2s} \tag{5}$$

where s is the aspect ratio of particles and the parameter τ is calculated by the equation (5). Both models are effective in estimating the Young's modulus of Cu matrix composites.

For the yield strength of Cu matrix composite, the modified shear-lag model can make good theoretical predictions [132, 133]:

$$\sigma_c = \sigma_m\left[1/2V_P\left(S + 2\right) + V_m\right]. \tag{6}$$

This model assumes that the presence of the ceramic particles does not impact the stress–strain response of the matrix, which allows the properties of the matrix to be incorporated into the model. Besides, the effect of particle sizes is not considered in this model. Recently, a micromechanics method has been widely used to predict the yield strength of composites, which is ascribed to several strengthening mechanisms including grain refinement strengthening, dislocation strengthening caused by CTE mismatch, load transfer strengthening and Orowan strengthening [134, 135]. This model can not only accurately predict the yield strength of composites but also provide a deep insight into the strengthening mechanism

Table 2. Summary of comprehensive properties of ceramics reinforced Cu matrix composites prepared by various processes. $\sigma_{0.2}$: yield strength; σ_{FS}: fracture strength; ε: fracture strain; CS: compressive strength; TS: tensile strength. MA: mechanical alloying; SPS: spark plasma sintering; IO: internal oxidation.

Composites (wt.%)	Preparation technique	$\sigma_{0.2}$ (MPa)	σ_{FS} (MPa)	ε (%)	CTE (10^{-6} K^{-1})	Electrical conductivity (% IACS)	Thermal conductivity (W mK^{-1})	References
3ZrO_2/Cu	MA	61 (CS)	310	44	—	73.45	—	[40]
6ZrO_2/Cu	MA	69 (CS)	346	43	—	14.17	—	
9ZrO_2/Cu	MA	72 (CS)	368	39	—	5.79	—	
12ZrO_2/Cu	MA	79 (CS)	385	35	—	1.65	—	
5.9Y_2O_3/Cu	MA + SPS	655 (CS)	932	33	—	53.8	—	[44]
1SiC/Cu	MA	48 (CS)	268	33	14.8	47.4	—	[9]
2SiC/Cu	MA	51 (CS)	283	32	14.1	42.9	—	
4SiC/Cu	MA	60 (CS)	312	27	12.9	37.9	—	
8SiC/Cu	MA	75 (CS)	340	21	11.2	16.7	—	
0.42Y_2O_3/Cu	MA + SPS	272 (TS)	296	12	—	—	—	[33]
3TiC/Cu	MA + SPS	572 (TS)	602	8	—	71.5	—	[43]
2.1WC/Cu	Pressureless sintering	244 (TS)	270	8	—	—	—	[102]
2.1WC/Cu	SPS	285 (TS)	310	11	—	—	—	
2.1WC/Cu	SPS + rolled	312 (TS)	361	12	—	—	—	
10SiC/Cu	SPS	110 (TS)	140	9	—	—	338	[103]
20SiC/Cu	SPS	68 (TS)	75	2.3	—	—	282	
10SiC/Cu	SPS + high-pressure torsion	395 (TS)	440	2.9	—	—	385	
20SiC/Cu	SPS + high-pressure torsion	385 (TS)	420	1.9	—	—	362	
2Al_2O_3/Cu	SPS (10 min) + hot extrusion	428 (TS)	510	14.7	—	87.1	—	[60]
2Al_2O_3/Cu	SPS (20 min) + hot extrusion	430 (TS)	497	11.5	—	83.2	—	
1Ti_2AlC/Cu	*In-situ*	118 (TS)	—	—	—	84.3	—	[104]
2Ti_2AlC/Cu	*In-situ*	132 (TS)	—	—	—	74.8	—	
3Ti_2AlC/Cu	*In-situ*	198 (TS)	—	—	—	50.5	—	
5Ti_2AlC/Cu	*In-situ*	241 (TS)	—	—	—	33.6	—	
1.1Al_2O_3/Cu	IO + hot-extruded	533 (TS)	570	25	—	85	—	[73]
1.8La_2O_3/Cu	IO + SPS	239 (TS)	349	37.6	—	93.1	—	[71]
0.34Al_2O_3/Cu	IO + high-velocity compaction	396 (CS)	443	—	—	81	—	[74]
0.34Al_2O_3/Cu	IO + hot pressing	281 (CS)	386	—	—	86	—	
0.34Al_2O_3/Cu	IO + hot extrusion	312 (CS)	378	—	—	87	—	
0.3 Y_2O_3/0.3Al_2O_3/ 0.3La_2O_3/Cu	IO	—	545 (TS)	—	—	93.5	—	[105]
2Al_2O_3/Cu	MA + extrusion + hot rolling	610 (TS)	648	6.2	—		—	[70]
1.6 Al_2O_3/Cu (R1)	IO + heat treatment	335 (TS)	387	6.6	—	95	—	[30]
1.6 Al_2O_3/Cu (R2)	IO + heat treatment	461 (TS)	522	8.2	—	90	—	

(Continued.)

Table 2. (Continued.)

1.5 Al_2O_3/Cu	IO + hot extruded	330 (TS)	358	17.1	—	—	—	[80]
1.1 Al_2O_3/Cu	IO	502 (TS)	563	—	—	—	—	[75]
0.2 Al_2O_3/Cu	IO	420 (TS)	458	—	—	—	—	[106]
0.12 Al_2O_3/Cu	IO	163 (TS)	220	11.8	—	89	—	[82]
0.6 Al_2O_3/Cu		261 (TS)	312	5.1	—	77	—	
12.1TiC/Cu	*In-situ*	183 (CS)	549	25.9	—	65.5	—	[98]
12.1TiC/Cu	*In-situ*	132 (CS)	526	35.7	—	55.6	—	
12.1TiC/Cu	*In-situ*	121 (CS)	417	34.9	—	40.3	—	
1TiC/Cu	*In-situ*	281 (CS)	584	35.8	—	77	—	[84]
11.2TiB_2/Cu	*In-situ*	168 (TS)	318	4.4	—	—	—	[95]
25.6 TiC + TiB_2/Cu	*In-situ*	949 (CS)	1239	7.1	—	—	—	[107]
34.1 TiC + TiB_2/Cu	*In-situ*	1003 (CS)	1252	5.8	—	—	—	
43.7 TiC + TiB_2/Cu	*In-situ*	1156 (CS)	1346	4.9	—	—	—	

of ceramic particles reinforced metal matrix composites. The final yield strength of the metal matrix composites is computed as the sum of the single strengthening contributions $\Delta\sigma_i$:

$$\sigma_c = \sigma_m + \sum\nolimits_i \Delta\sigma_i. \tag{7}$$

Generally, the particles uniformly dispersed in matrix effectively impede dislocation motions, and fine-grained particles provide strong barriers to grain boundary migration via the Zener pinning mechanism [136],

$$d_m = \frac{4\alpha D_p}{3V_p} \tag{8}$$

where d_m is the grain size of matrix, α is the proportionality constant, and D_p is the dimensions of particles. The resulting grain refinement reduces the formation of defects and improve crack propagation resistance. The contribution of grain refinement strengthening could be formulated using the classical Hall–Petch theory:

$$\Delta\sigma_{HP} = \frac{k}{\sqrt{d}} \tag{9}$$

where k is a constant and d is the mean grain size.

In addition, owing to the discrepancy in the physicochemical properties of the ceramic particles and the Cu matrix, the ceramic second phase would induce dislocation pinning and accumulation at the interface, which results in dislocation strengthening. The effect caused by dislocation is expressed as [137]:

$$\Delta\sigma_{CTE} = \alpha Gb\left(\frac{12\Delta T\Delta C V_p}{bd_p}\right)^{1/2} \tag{10}$$

where ΔT is the difference in temperature and ΔC is the difference in CTE between the matrix and the ceramic particles; G refers to the shear modulus of the matrix and b is Burger's vector; d_p represent the mean diameter of reinforcing particles.

When the particles size is relatively fine (<100 nm), the Orowan strengthening mechanism is also prominent [138]. The Orowan strengthening effect is modeled as [139, 140]:

$$\Delta\sigma_{Orowan} = M\frac{0.4Gb}{\pi(1-\nu)^{1/2}}\frac{\ln(D/b)}{\lambda} \tag{11}$$

where M is orientation factor on average, ν is Poisson's ratio, λ is the nanoparticle spacing, and D is the nanoparticle average grain size.

The resulting bending of dislocations would increase the lattice distortion energy in the area affected by the dislocation, increasing the resistance to the movement of the dislocation line and the resistance to slippage. From the TEM images illustrated in figures 10(a)–(d) [126], the Y_2O_3 particles remain stable in the Cu matrix during the sintering process, and the Y_2O_3 particles do not react with the Cu matrix. Besides, the good interfacial bonding between Y_2O_3 particles and the Cu matrix significantly enhances the mechanical performance of the composites and minimizes the impact on their thermal and electrical conductivity. The electron backscatter diffraction (EBSD) results of the Cu matrix composite are illustrated in figures 10(e)–(h) [59]. For the composite samples, the microstructure consists of equiaxed grains with uniform dimensions, which are the result of grain growth and static recrystallization in the sintering process. The grain orientations of the two samples can be considered random. Nanoparticles penetrate the Cu grain boundaries and pin the Cu grains, thereby preventing grain growth based on the Zener mechanism. Besides, the high strain generated by the reinforcements in the Cu matrix promotes the recrystallization process at high temperature therefore delays the strain release, which is the driving force for grain growth at high temperature. Therefore, the composites have significantly smaller grain size than the pure Cu.

In addition to the grain refinement strengthening, dislocation strengthening and Orowan strengthening, the load transfer strengthening mechanism between the softer matrix (Cu matrix) and the harder nanoparticles (ceramic phase) also comes

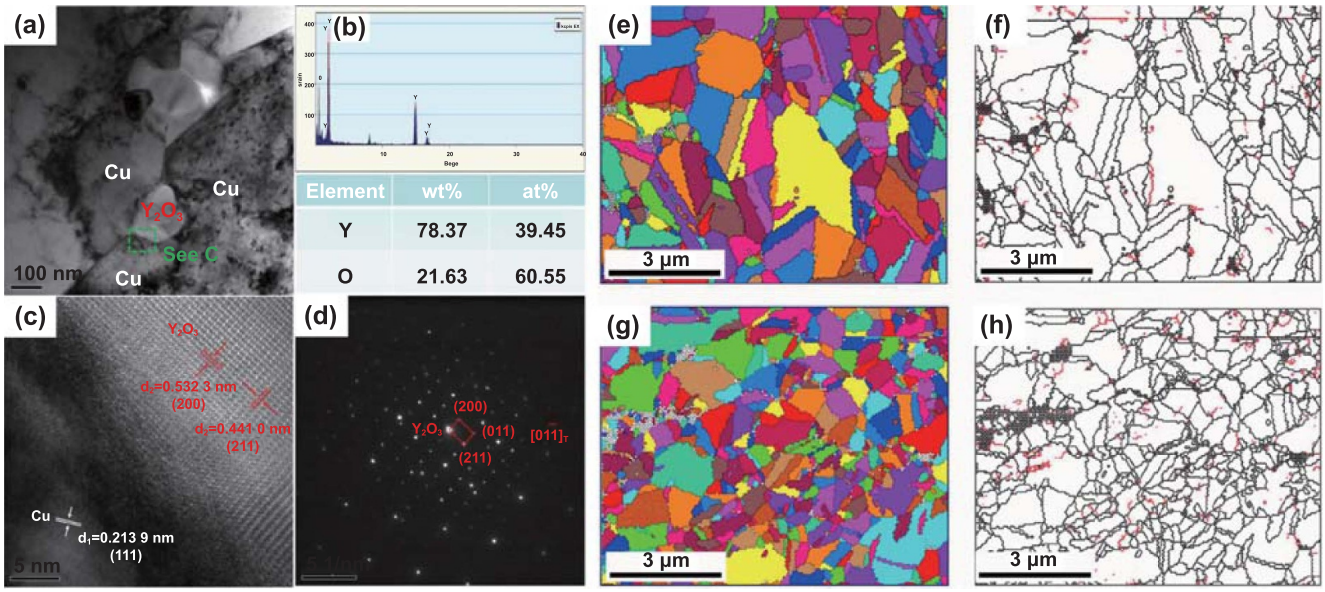

Figure 10. Microscopic characteristics of ceramic particles and grain structure of the matrix in Cu matrix composites. (a) TEM image of the 3 wt.%Y_2O_3/Cu composite. (b) EDS mapping and elemental specific gravity of the particle in (a). (c) HRTEM image of the green dashed box in (a). (d) the corresponding selected diffraction in (c). Reprinted from [126], Copyright (2021), with permission from Elsevier. EBSD maps of the samples: (e), (f) Cu and (g), (h) nanostructured Cu reinforced with SiC and CNT. Reprinted from [59], Copyright (2020), with permission from Elsevier.

into play when external loading is applied [141]. Nardone and Prewo [142] presented a modified model to describe the strengthening effect of load transfer:

$$\Delta\sigma_{\mathrm{LT}} = V_{\mathrm{p}}\sigma_0\left[\frac{(l+t)A}{4l}\right] \tag{12}$$

where σ_0 is the yield strength of the matrix, l and t are the dimensions of the particles in the direction parallel and perpendicular to the load, respectively. Generally, for the composite with high content of ceramic particles, the force transfer process would be the main strengthening mechanism. As shown in figure 8(f), the finite element modeling (FEM) based on the three-dimensional representative volume element (RVE) of real microstructure was employed to investigate the stress distribution inside the composite under loading [100]. The results clearly show that the average stress on particles is several times higher than that of the matrix, which demonstrates that the ceramic particles carry most loadings. The uniformly dispersed ceramic particles greatly enhance the mechanical properties of the composite. However, a large stress concentration occurs at the tip of the particle. Thus, fracture occurs at that location and then initiates cracks in the matrix, resulting in failure of the composite. As such, the morphology of ceramic particles greatly affect the performance of the composite. This will be further discussed in the next section.

3.2. Effect of ceramic particles on the thermal expansion coefficient of Cu matrix composites

For the CTE of ceramic reinforced Cu matrix composite, the inherent performance of the matrix material and the reinforcement phase and their interaction directly determine the CTE of the composite. So far, a series of work has been conducted on the thermal expansion behavior of metal matrix composites through experimental investigations and theoretical calculations, which results in several reasonable calculation models to more accurately predict the CTE of different composites [125, 143–145].

(1) ROM model

The ROM model is a simplest mixed rule, which is expressed as:

$$\alpha_{\mathrm{c}} = \alpha_{\mathrm{m}}V_{\mathrm{m}} + \alpha_{\mathrm{p}}V_{\mathrm{p}} \tag{13}$$

where α is the CTE. This model is suitable for composites with similar modulus differences of components, which is the result given by ignoring the elastic interaction between components.

(2) Turner model

The Turner model takes into account the effect of hydrostatic stress on adjoining phases, which is expressed as:

$$\alpha_{\mathrm{c}} = \frac{\alpha_{\mathrm{m}}V_{\mathrm{m}}K_{\mathrm{m}} + \alpha_{\mathrm{p}}V_{\mathrm{p}}K_{\mathrm{p}}}{V_{\mathrm{m}}K_{\mathrm{m}} + V_{\mathrm{p}}K_{\mathrm{p}}} \tag{14}$$

where K is the bulk modulus and $K = \frac{E}{3(3-E/G)}$; E is the elasticity modulus. Compared to the ROM model, the Turner model assumes that no internal stress exists in the composite and that the deformation degree of each component of the composite is the same.

(3) Kerner model

The Kerner model is currently the most used theoretical formula to calculate the CTE of metal matrix composites with particle reinforcement, which includes the shear strain in particulate composites,

$$\alpha_c = \alpha_p V_p + \alpha_m V_m + (\alpha_p - \alpha_m) V_p V_m \times \frac{K_p - K_m}{V_p K_p - V_m K_m + 3K_p K_m / (4G_m)} \quad (15)$$

where G is the shear modulus. This model utilizes a classical self-consistent method to predict the CTE of composites. It assumes that the intermediate reinforcement particles of the composite material are spherical and the outer layer is uniform matrix, and there exist both shear force and isostatic pressure in each phase of the composite.

(4) Eshelby model

The Eshelby model, also known as the equivalent inclusion model, is also a classical method for calculating the CTE of composite.

$$\alpha_c = \alpha_m - V_m\{(C_m - C_P)[S - V_m(S - N)] - C_m\}^{-1} \times C_p(\alpha_p - \alpha_m) \quad (16)$$

where S is the Eshelby tensor, C is the stiffness and N is the matrix tensor corresponding to the reinforcement. The model assumes that both the matrix and the ceramic phase are isotropic in expansion and the model can more accurately estimate the CTE of the composites.

The above theoretical models have been widely applied to the design and preparation of composites. Moreover, all these models clearly reflect that the content of ceramic phase directly affects the CTE of the composites. The CTE tends to decrease with increasing the ceramic content. However, the initial assumptions of each model have certain defects and cannot fully objectively reflect the actual internal conditions of metal matrix composites. These models show different prediction accuracy for different types of metal matrix composites. Therefore, the predicted CTE values of metal matrix composites are often different from the actual results because the effects of non-uniform stress distribution, thermal residual stress, matrix plastic deformation, etc on the thermal expansion behavior of composites are not considered. Fei *et al* [146] pointed out that the CTE of composites is closely associated with the rate of change of thermal residual stress and dislocation density of the matrix. Due to the large CTE differences between the ceramic phase and the metal matrix, all the metal matrix contains thermal residual stress. When different heat treatment processes are applied to the composites, both the dislocation density and thermal stress of the composites prepared by slow cooling are lower than the corresponding ones of the composites prepared in fast cooling (water quenching) condition. The composites after quenching demonstrates much different thermal expansion behavior compared with the counterparts by slow cooling (figures 11(a)–(d)). The CTE curve as a function of temperature of quenched composite shows a minimum peak and a maximum peak, while there is no maximum peak for composite prepared under slow cooling. This can be ascribed to the thermal elastic relaxation and plastic relaxation of the matrix during the CTE test, and the rate of change of thermal residual stress directly determines the CTE of the composite. Therefore, the microstructure and thermal stress in the matrix have significant influences on the thermal expansion behavior of the metal matrix composite. In fact, the size and morphology of the particles, as well as the complex stress–strain state inside the matrix, also have a great impact on the CTE of the composites. Non-uniform stress distribution would lead to non-uniform thermal expansion behavior of the composite, which is difficult to predict by theoretical calculations. The microstructure defects such as pores, reaction products, interface debonding, and agglomeration of ceramic particles would also inevitably affect their thermal expansion behavior. Therefore, novel micromechanical models are needed to reflect the CTE of composites.

On this basis, FEM is an effective strategy to perform deep analyses on the experimental results of the composite microstructure with respect to particle characteristics, thermal residual stress, interfaces, holes, etc to study the complex thermal expansion behavior [148–151]. The detailed stress and strain distribution and deformation can be visualized in the RVE model, which provides a more accurate prediction of the CTE for metal matrix composites. Sharma *et al* [147] constructed the RVE models according to the actual microstructure of composite to evaluate the effect of thermal residual stress on CTE, as illustrated in figures 11(e)–(h). By studying the temperature-dependent linear elastic and elastoplastic matrix material behavior, they found that the presence of thermal residual stress affects the effective CTE in the heating process. The contact status of the reinforcing particles greatly impact the thermal expansion behavior of the composite. The predicted CTE using RVE with overlapping microstructure is in accordance with the measured CTE. For RVE with separated or contact particles, the predicted CTE is higher than the experimental one. The presence of voids reduces the effective CTE of the metal matrix composite. Compared to the theoretical calculations, FEM provides a more intuitive prediction from a microscopic perspective [152, 153]. The effects of non-uniform stress distribution, thermal residual stress, matrix plastic deformation and microstructure defects in the composite are comprehensively considered through reasonable modeling methods [154]. Therefore, the FEM tends to show more accurate predictions.

3.3. Effect of ceramic particles on the conductivity of Cu matrix composites

While effectively improving the strength and CTE of the Cu matrix, it is also important to maintain good conductivity. For metal matrix composites, the thermal and electrical conduction process is determined by the matrix and the reinforcing phase. In metals, electron conduction is the main heat transfer mechanism; while for ceramics, the conduction mechanism is mainly phonon conduction. In comparison, the conductivity of

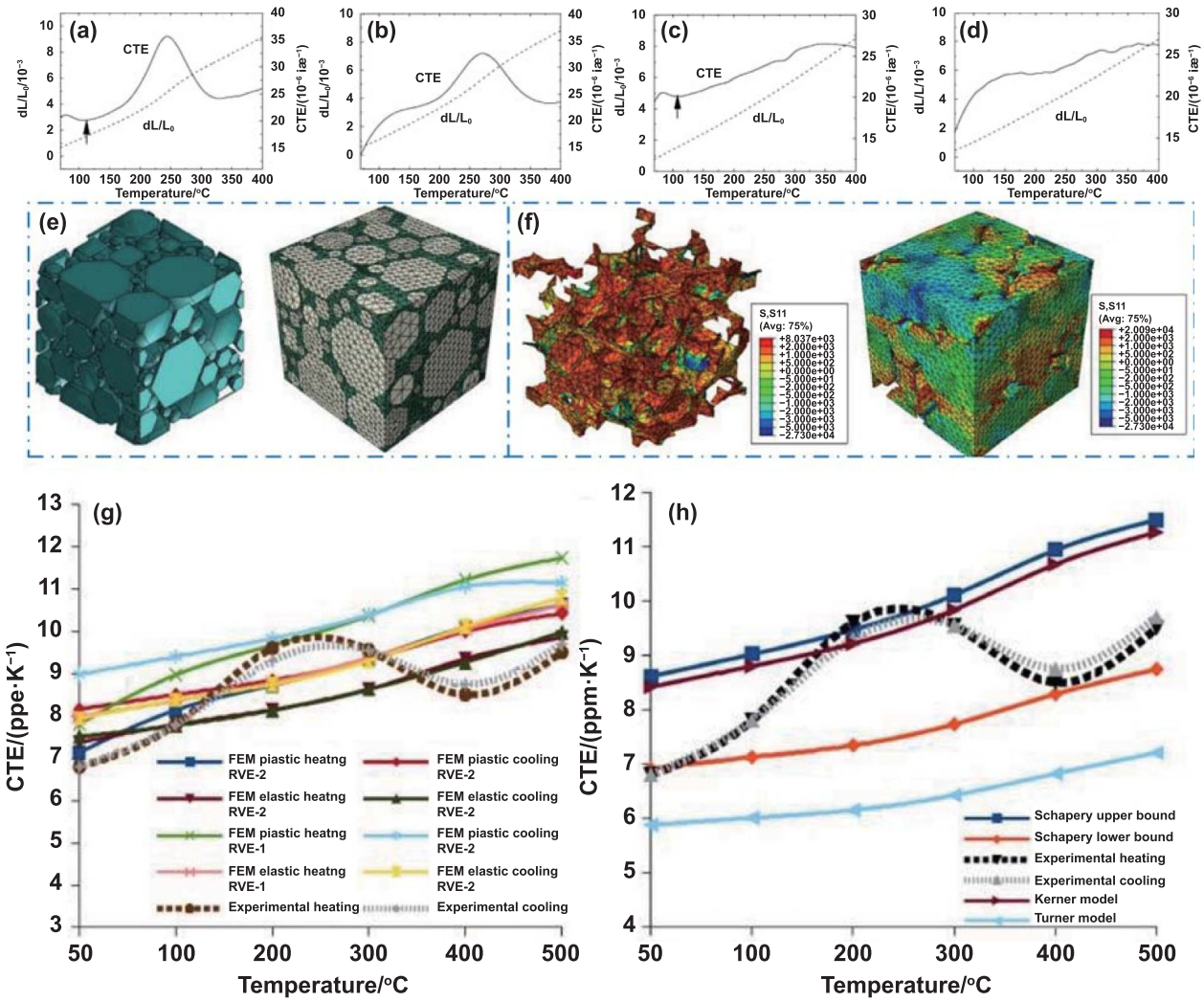

Figure 11. Thermal expansion behavior of ceramic particles reinforced metal matrix composites. Relative elongation and CTE as a function of temperature for the quenched SiC/Al composite with the heating rate of 2.5 °C min^{-1} (a) and 8 °C min^{-1} (b). Relative elongation and CTE as a function of temperature for the slowly cooled SiC/Al composite with the heating rate of 2.5 °C min^{-1} (c) and 8 °C min^{-1} (d). Reprinted from [146], Copyright (2003), with permission from Elsevier. (e) FE model of 70 vol.% SiC/Al composite. (f) Thermal residual stresses (S11, MPa) distribution in Al matrix and SiC phase of 70 vol.% SiC/Al composite. (g) FE modeled total CTE of 70 vol.% SiC/Al composite with no stress state at room temperature (h) predicted CTE by analytical micromechanical models of 70 vol.% SiC/Al composite. Reprinted from [147], Copyright (2016), with permission from Elsevier.

ceramics in metal matrix composites is negligible and the presence of ceramics largely hinders the electronic conductivity in the metal matrix. The conductivity of composite is affected by microstructural features such as the type and volume fraction of the ceramic phase, particle size, and interfacial barrier. In fact, the matrix of the composite is the main conduction path and metal conduction mainly relies on current carrier electron transmission. Lattice defects, impurities and lattice vibrations in the matrix would scatter free electrons, which is similar to the process of electronic heat transfer. As a result, the electrical conductivity of metal is approximately proportional to the thermal conductivity. The metal electronic thermal conductivity (γ_e) and electrical conductivity (η) can be related by:

$$L_0 = \frac{\lambda_e}{\eta_T} = \frac{\pi^2}{3}\frac{\lambda_B}{e^2} \tag{17}$$

where λ_B is the Boltzmann constant, and L_0 is a constant, known as the Lorentz constant. In order to more directly reflect the effect of reinforcement particles on the conductivity of the metal matrix, the following theoretical models are commonly employed to predict the thermal conductivity of metal matrix composites [125, 155]. Herein, the electrical conductivity of composite is proportional to its thermal conductivity, so it will not be described here.

(1) Maxwell model

The Maxwell model is the most classic theoretical model for predicting the thermal conductivity of composites, which is expressed as:

$$\gamma_c = \gamma_m \frac{2(1-V_p) + (\gamma_p/\gamma_m)(1+2V_p)}{(2+V_p) + (\gamma_p/\gamma_m)(1-V_p)} \tag{18}$$

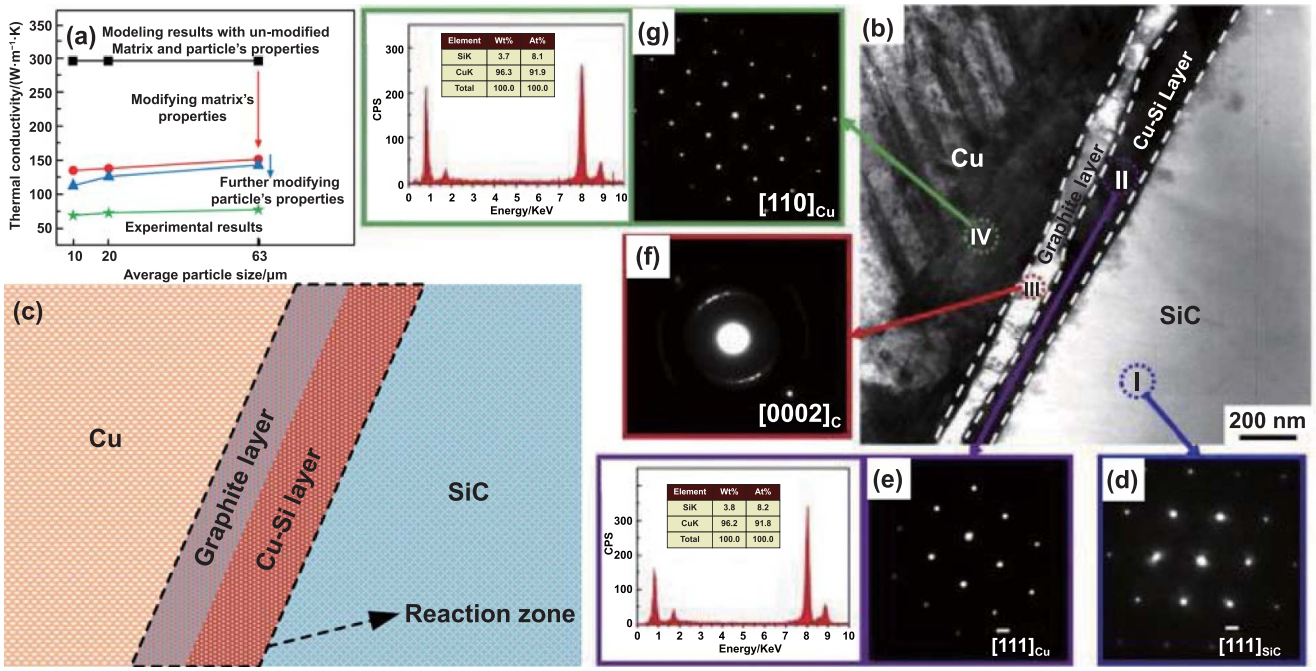

Figure 12. CTE results and interfacial structure of SiC/Cu composite. (a) Comparison of experimental and computational CTE results based on Hasselman–Johnson model for SiC/Cu composites. (b) TEM image; (c) schematic diagram of (b); SAED patterns of (d) I area, (e) II area, (f) III area and (g) IV area. Reprinted from [157], Copyright (2014), with permission from Elsevier.

where γ is the thermal conductivity. This model assumes that the reinforcement particles are spherical, and it ignores the effect of interfacial thermal resistance on the thermal conductivity of the composite. This model takes into account the thermal conductivity of both the matrix and the reinforcing phase in the composite and the effect of the reinforcing phase content on the thermal conductivity of the composite material.

(2) Hasselman–Johnson model

The Hasselman–Johnson model, also known as effective medium approximation, is expressed as:

$$\gamma_c = \gamma_m \left[\frac{2(1-V_p) + (\gamma_p/\gamma_m)(1+2V_p) + 4(\gamma_p/Dh)(1-V_p)}{(2+V_p) + (\gamma_p/\gamma_m)(1-V_p) + 2(\gamma_p/Dh)(2+V_p)} \right] \tag{19}$$

where D is the diameter of the reinforcement, h is the thermal boundary conductance. This model takes into account the influence of interfacial thermal resistance and particle dimensions on thermal conductivity. Interfacial thermal resistance is caused by physical differences between phases, defective mechanical or chemical adhesion at the interface, and mismatches in the CTE.

If $D \to \infty$, equation (19) is the equation of Maxwell model, which is equivalent to ignoring the interface thermal barrier.

Setting $D \to 0$, equation (19) becomes:

$$\gamma_c = \gamma_m \frac{1-V_p}{1+0.5V_p} \tag{20}$$

where V_p equals the porosity. This is equivalent to the situation where the particles in the metal matrix are pores.

The above theoretical models have been well applied in a large number of studies [125, 156]. The prediction results by theoretical models can well reflect the heat transfer capacity of the metal matrix composite and explore the effect of various factors on the thermal conductivity. Moreover, like the prediction model for CTE, ceramic content is also the most important influencing factor, and the conductivity decreases as increasing the ceramic content. In addition, the theoretical values of the metal matrix composite calculated by the models often differ from the experimental results. The initial assumptions of each model still have certain defects, and the actual internal conditions of metal matrix composites cannot be fully and objectively reflected by theoretical models. Therefore, the thermal conductivity of Cu matrix composites is usually far below the theoretical expectations [157]. The work of Molina *et al* [158] and Chu *et al* [159] pointed out that the actual thermal conductivity of Cu decreases from 389 W $(m{\cdot}K)^{-1}$ to about 70 W $(m{\cdot}K)^{-1}$ due to the scattering of electrons by the crystal defects, sub-grains and lattice distortion induced by dissolved solute element in matrix. The selected area electron diffraction (SAED) patterns shown in figure 12 also demonstrate that the Si element is solidly soluble in the Cu–Si layer and Cu matrix. Although considering the low thermal conductivity of the matrix, the theoretical results are still higher than the actual results, as shown in figure 12(a). There are still other factors that govern the thermal conductivity of composites. As shown in figures 12(b) and (c), interfacial reactions have occurred and an evident graphite layer and Cu–Si layer appear between the Cu matrix and SiC phase. This induces high interfacial thermal resistance and leads to low thermal conductivity of SiC/Cu composites.

In conclusion, there are many factors that affect the conductivity of composites. The refined grain size increases the area of grain boundary and phase boundary in the composite, which would intensify the interfacial scattering to electrons and hence decrease the conductivity of composite. Besides, the residual stress and plastic strain in the composite caused by the difference of CTE between the ceramic particles and metal matrix also negatively affect its conductivity. On this basis, research and development of the more applicable and comprehensive theoretical models is also one of the future research directions. Notably, the MAX phase as an advanced ceramic material is a competitive reinforcement in Cu matrix composites [160, 161]. These ternary carbides or nitrides (e.g. Ti_3AlC_2, Ti_3SiC_2, etc) combine the properties of ceramics and metals, exhibiting high conductivity, mechanical properties, good thermal shock resistance, excellent oxidation resistance and corrosion resistance owing to their unique atomic bonding and crystalline structure [162–165]. Recently, extensive work has been done to explore the preparation process and the conduction and mechanical properties of Cu-MAX composites. The results show that the MAX phases are efficient to strengthen the mechanical properties of Cu matrix composites, without a drastic reduction of their conductivity [166–168]. Nevertheless, the research of Cu-MAX composites is still in its infancy, and more in-depth research and exploration are urgently needed.

4. Effect of ceramic characteristics on the properties of Cu matrix composites

As mentioned above, the introduction of ceramic particles could directly affect the stress distribution, conduction and thermal expansion behavior of the Cu matrix. The essential characteristics of the ceramic particles would also have an impact on the comprehensive performance of composites. However, most of the aforementioned theoretical models only consider the ceramic content in the composites, and it is difficult to predict the effect of other factors of particles on the performance of the composites through the theoretical models. Therefore, the most important influencing factors such as the content, size and morphology of the ceramic particles and the interface between the matrix and the reinforcement are further reviewed below.

4.1. Ceramic particle content

It was reported [19, 169] that the content of ceramic phase directly determines the comprehensive properties and the potential application fields of Cu matrix composites. As shown in figure 13, as the ceramic content increases, the strength of the composites tends to increase to a certain degree, by sacrificing the ductility. The FEM results [170] also demonstrated that both the elastic modulus and yield strength of the TiB_2/Cu composites increase with increase in the particle content while the elongation decreases, as illustrated in figure 14(a). Figures 14(b) and (c) show the total stress and average stress on the ceramic particles with different particle contents. The total stress on particles increases with the increase in the particle content, while the average stress on particles is maintained approximately the same. Therefore, the ceramic particles with higher content can sustain the load more effectively and enhance the strength of the composite. However, as the ceramic particle content increases, the spacing between ceramic particles gradually decreases and a large amount of aggregation takes place. As shown in figures 14(d) and (e), large areas of interfacial damage occur in the RVEs, and the damage area of the Cu matrix increases with the increase of particle content. This results in more pronounced stress concentration in the Cu matrix and the composites with high particle content are more prone to microcracking and rapid propagation into the main cracks. Therefore, the load is not effectively transferred from the matrix to the ceramic particles, which reduces the ductility of the composite.

With regard to the CTE and conductivity, the content of ceramic particles performs a crucial role in determining the CTE and conductivity of ceramic particle reinforced Cu matrix composites. As described in sections 3.2 and 3.3, both the CTE and conductivity of composites decrease as increasing the ceramic content. However, the increase of ceramic content in the composite tends to cause agglomeration of particles, which largely weakens the strengthening effect of particles. Accordingly, a more suitable ceramic content is required to obtain superior comprehensive properties (i.e. maintaining a good combination of mechanical performance and CTE and conductivity) under different preparation processes.

4.2. Ceramic particle size

In the process of introducing ceramic particles into a metal matrix, the size of the ceramic particles also has a great influence on the comprehensive performance of the composite. Appropriate particle size is of great significance to further optimize the comprehensive performance of metal matrix composites. Generally, the size of ceramic particles can be classified into micron (1–100 μm), submicron (0.1–1 μm) and nanoscale ($<$100 nm). As shown in figure 15, the vicinity of micron particles is beneficial to form particle deformation zone, and the area with high dislocation density can be generated surrounding submicron particles due to pinned dislocations and deformation mismatch between the matrix and the particles. Meanwhile, the introduction of fine particles (i.e. in nanoscale or submicron) may delay or impede grain growth via a pinning effect on the grain boundaries [171]. However, when micron-sized or nano-sized particles are introduced into the metal matrix composites, the high particle content can easily lead to particle agglomeration, which significantly deteriorates the strength and ductility of the composite. Compared with the micron-sized particles, the nano-sized particles in metal matrix has much higher agglomeration propensity owing to the large specific area and van der Waals force. The mixture of micron-sized and nano-sized particles was reported to have a more apparent strengthening ability than monolithic size particles [172, 173].

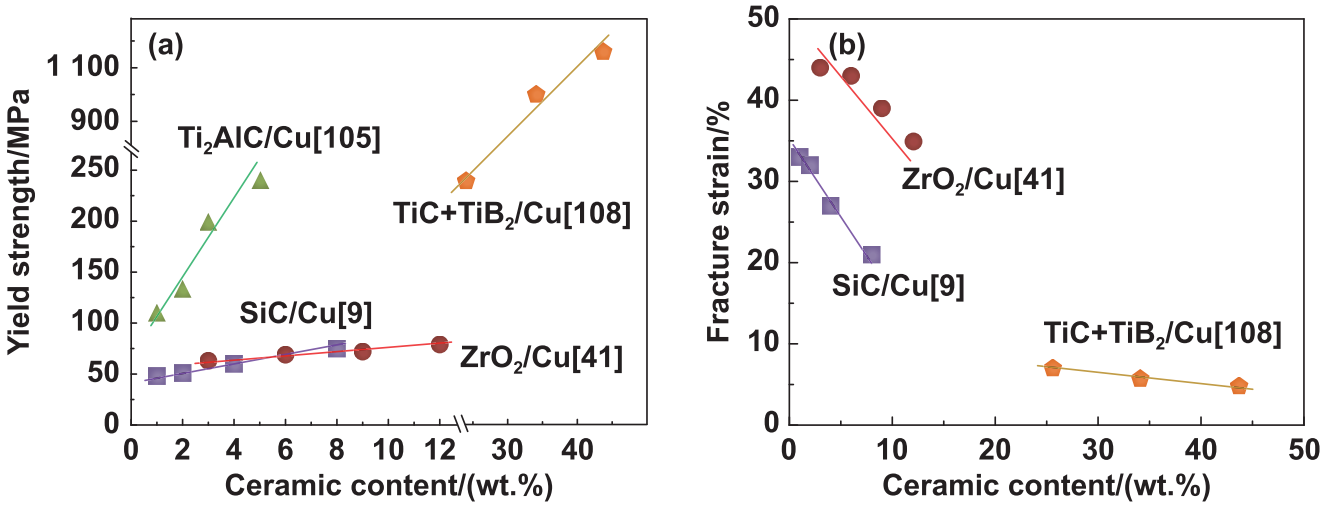

Figure 13. Linear relationship between the mechanical properties and ceramic content of ceramic reinforced Cu matrix composites. (a) Yield strength versus ceramic content; (b) fracture strain versus ceramic content [9, 40, 104, 107].

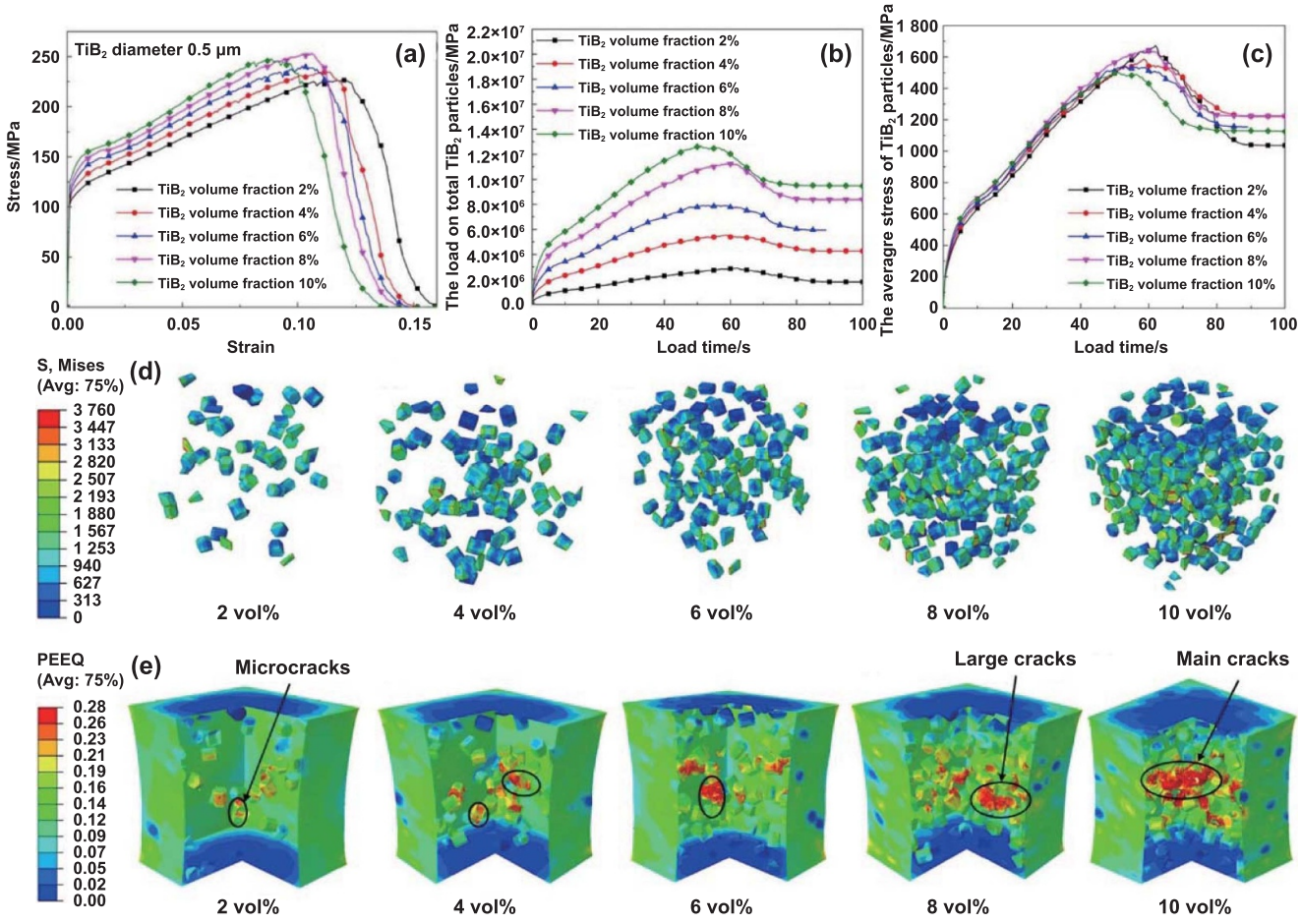

Figure 14. FEM results investigating the effect of particle content on the mechanical response of composites. (a) The simulated stress–strain curve of TiB_2/Cu composites with different particle contents. The (b) total stress and (c) average stress on particles. (d) Mises stress of particles and (e) equivalent plastic strain of Cu matrix in the composites with different particle contents. Reprinted from [170], Copyright (2022), with permission from Elsevier.

Tian *et al* [174, 175] successfully prepared bimodal-sized (micron + nanoscaled) TiC/Al–Cu composites by incorporating micro-sized and nano-sized TiC. The composites with bimodal-sized TiC possess higher strength, ductility and creep resistance compared with the composites with monomodal-sized particles, which is ascribed to more significant precipitation strengthening and grain refinement of the bimodal-sized particles.

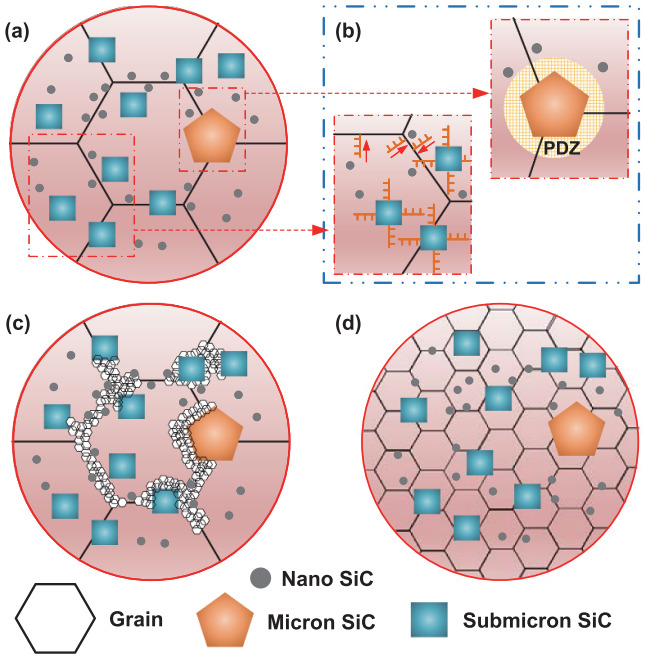

Figure 15. Schematic illustration of dynamic recrystallization affected by SiC size during hot extrusion: (a) the microstructure before hot extrusion. (b) High density dislocations surrounding submicron SiC and particle deformation zone surrounding micron SiC. (c) Dynamic recrystallization nucleuses priority occur around SiC and at grain boundaries. (d) The microstructure after dynamic recrystallization. Reprinted from [171], Copyright (2016), with permission from Elsevier.

When a metal matrix composite contains only single-scale particles and the particles are evenly distributed, the composite with relatively smaller particle size demonstrates better mechanical properties. Owing to the difference in CTE between the ceramic particles and the matrix, local deformation in the interfacial region and high-density dislocations are produced in the composites during the preparation process, leading to dislocation strengthening. When the content of the reinforced particles is constant, the increased dislocation density around the particles and the strain gradient are noted in the composite with smaller particle sizes. Such a phenomenon further enhances the dislocation strengthening effect of the composite, thereby increasing its load-bearing capacity. Ma *et al* [176] simulated the effect of particle size on the tensile behavior of composites by establishing the microstructure-based RVE models. The simulated stress–strain curves with different particle sizes are shown in figures 16(a) and (b), and the average S11 (stress in the X-axis) stress of Al_3Ti particles and metal matrix are compared in figure 16(c). For the same content of particles, the yield strength and elongation of the composite are enhanced slightly as decreasing the particle size. Meanwhile, the Al_3Ti particles with smaller size can bear higher S11 stress during the initial deformation. After further loading, the stress on particles remains constant, while the strength of the matrix keeps increasing. Therefore, smaller particles tend to 'be strengthened' faster and bear higher mean stress than the larger particles. Figure 16(d) shows the damage of the matrix at different moments of strains. Under the same nominal strain, the damage in the matrix with small particles evolves slowly and uniformly, while the damage extends rapidly surrounding the large ones. Therefore, cracks are always initiated adjacent to large particles in the aggregation area, due to that large particles are more prone to deformation and lead to stress and strain concentrations. Likewise, Yan *et al* [177] conducted the similar study using FEM in combination with Taylor-based theory of nonlocal plasticity. Both numerical and experimental results indicated that the flow stress and work hardening rate of the composites increase as decreasing the particle size when the content of the reinforcements is constant. This is mainly attributed to the fact that the strain gradient in the matrix increases as the particle size decreases.

Furthermore, the thermophysical performance and electrical conductivity of metal matrix composites are also closely associated with the size of reinforced particles. Generally, the increase in particle size in metal matrix composite would increase its CTE, thermal conductivity and electrical conductivity [125, 157, 178, 179]. The decrease in particle size increases the dislocation density of the matrix, which increases the yield strength of the composite. On this basis, the thermal stress generated in the heating process is more difficult to relax and the thermal residual stress in the composite increases, which hinders the thermal expansion of the matrix. Therefore, as the particle size decreases, the CTE of the metal matrix composite decreases. At constant particle content, smaller particle size leads to more particles and smaller particle spacing in the composite, which can more effectively hinder the expansion of matrix at high temperature. Thus, small particle size in a composite would significantly reduce the increase rate of CTE with temperature [180].

For the conductivity of metal matrix composites, Efe *et al* [181] compared the influence of different contents and sizes of SiC particles on the relative density and electrical conductivity

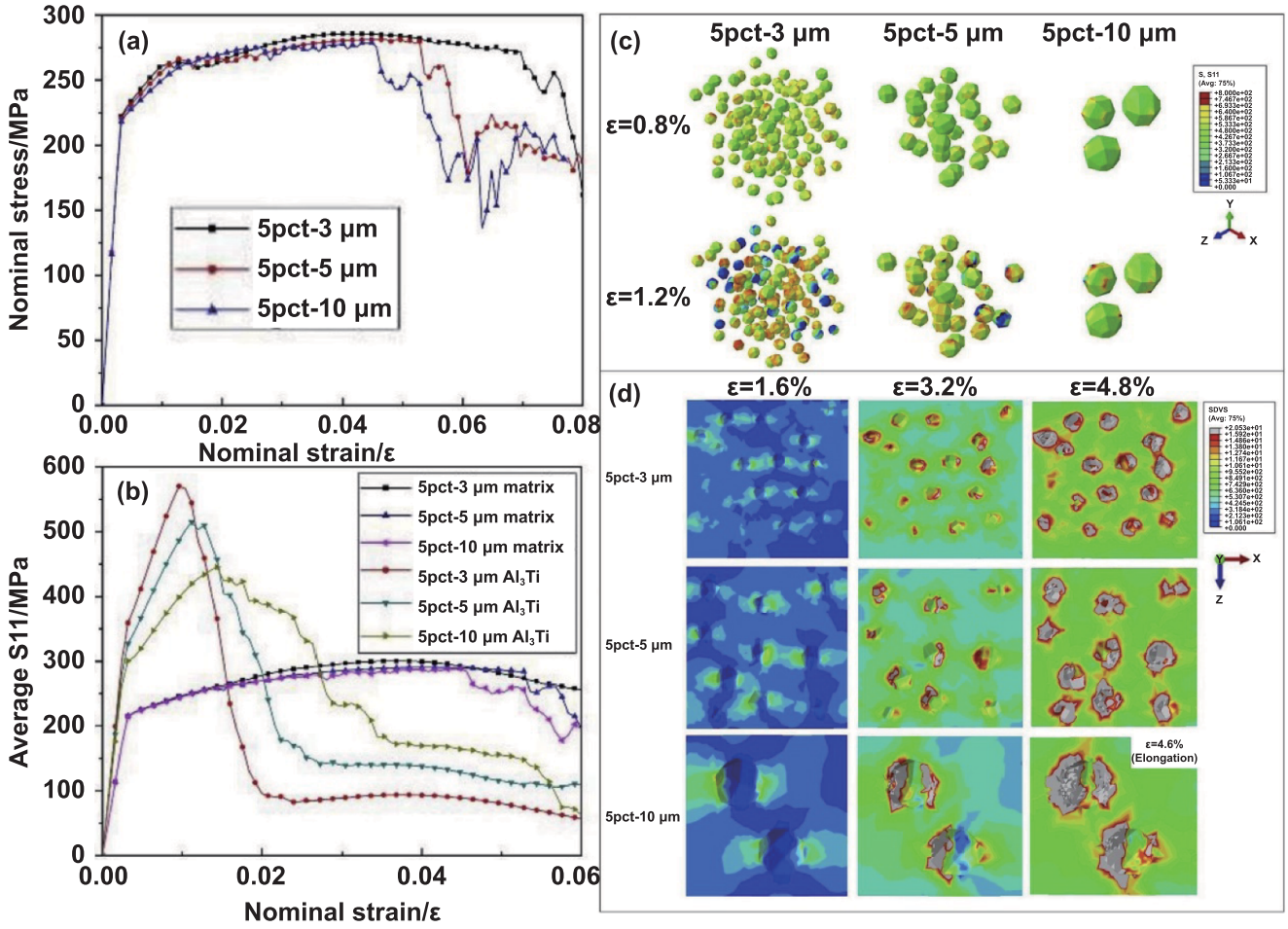

Figure 16. FEM results investigating the effect of particle size on the mechanical response of composites. (a) The simulation stress–strain curves for Al_3Ti/A356 composites. (b) The average S11 stress of Al_3Ti particles and A356 matrix at different particle sizes, respectively. (c) Stress distributions on particles at different particle sizes. (d) Damage distribution of the matrix at different particle sizes. Reprinted from [176], Copyright (2019), with permission from Elsevier.

of Cu matrix composites. As shown in figure 17, the relative density and electrical conductivity of SiC/Cu composites increase as increasing the SiC particle size. In fact, the thermal conductivity and electrical conductivity of the material mainly depend on the movement of electrons in the matrix. However, the existence of insulating ceramic particles and scattering at the interface hinder the movement of electrons. With the decrease in particle size, the hindrance effect of particles is further aggravated and the interface proportion between particles and matrix increases, which significantly reduces the thermal and electrical conductivity of composites.

4.3. Ceramic particle morphology

During the preparation of Cu matrix composites, the morphology of the ceramic particles also directly affects the stress distribution of the surrounding metal matrix, which then reflects the difference in the mechanical performance of the composites. In general, the failure mode of a composite varies as modifying the particle morphology. Compared with the spherical particles, the reinforcement particles with sharp corners are more effective in pinning dislocations and have the stronger initial strain strengthening effect in composites [182, 183]. The higher load-bearing capacity is provided by the angular particles. However, both experimental and numerical simulation results [98, 183] indicated that voids tend to nucleate preferentially at the corners of the particles when the composite is loaded. Therefore, the metal matrix composites reinforced with spherical particles have larger ductility but slightly lower yield strength and work hardening rate are than those reinforced with angular particles.

Wu *et al* [151] developed a novel model of composite with realistic microstructure to investigate the effect of particle morphology and distribution on the deformation behavior of metal matrix composites. The deformation of the matrix is concentrated near the crack tip, which results in the destruction of the matrix when its equivalent plastic strain reaches a threshold value. As shown in figures 18(a) and (b), the cracks propagate along the direction of high stress in the matrix. Microcracks of the particles occur at corners, in which stress concentrations are prone to occur, and the matrix breaks near the crack tips. Then, the main crack passes through the

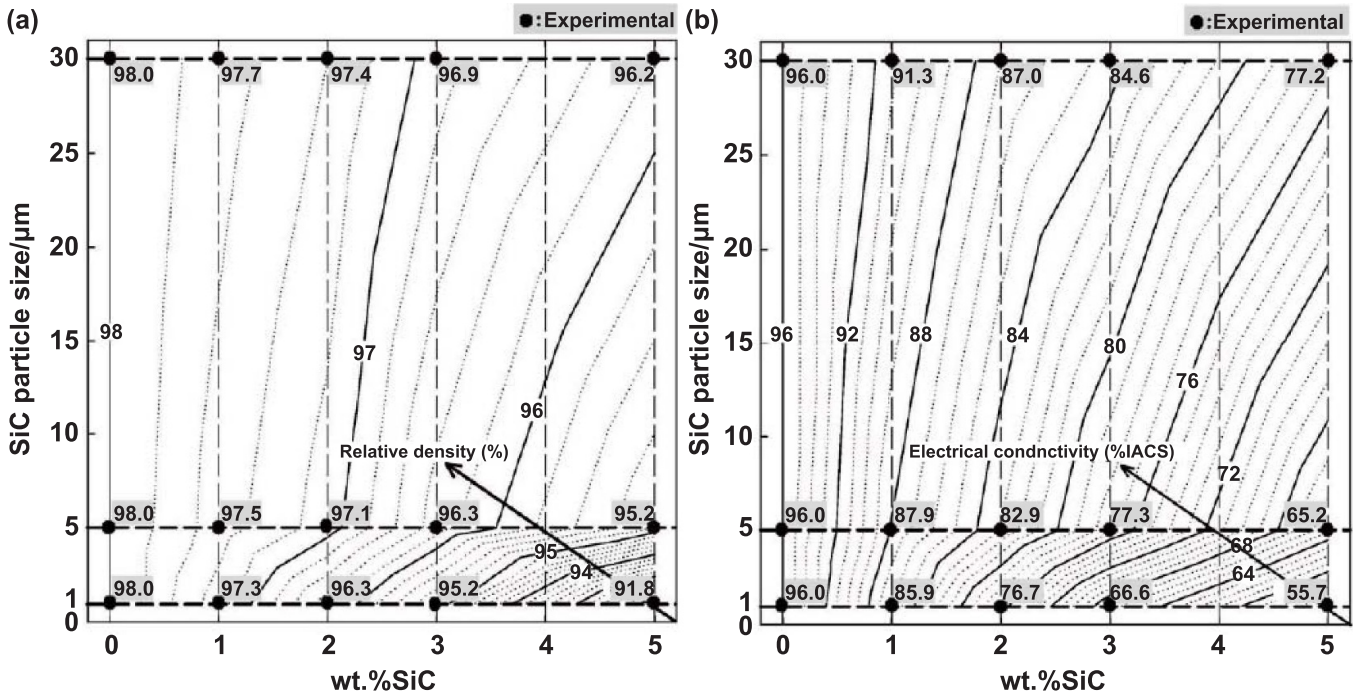

Figure 17. Contour diagrams illustrating the properties of SiC/Cu composites as a function of SiC content and particle size. (a) Relative density versus SiC content and particle size; (b) electrical conductivity versus SiC content and particle size. Reprinted from [181], Copyright (2012), with permission from Elsevier.

particle agglomeration zone where microcracks are accumulated, while no significant particle debonding is detected and few particles fracture along the crack side (figures 18(c)–(f)). The change of the ceramic particle morphology affects the stress–strain response of the composites and the stress–strain distribution of the surrounding matrix [184, 185]. As shown in figure 18(g), with the increase in particle roundness, both the elastic modulus and yield strength of the composite decrease, while the fracture stress and strain increase. This is attributed to that the stress concentration generated at the sharp corners facilitates the improvement of elastic modulus and yield strength in the metal matrix. However, after yielding, the stress concentration at the sharp corners of the particle leads to premature softening and cracking of the matrix. As seen from figures 18(h)–(j), when the particles have larger roundness, the stresses at the sharp corners of TiB_2 particle are closer to the internal stresses, the stress distribution on the particles is more even, which obviously optimizes the stress concentration at the corner [170].

In metal matrix composites with the same particle content, type and size, the particle morphology has little effect on the conductivity and CTE of the composites. Generally, the influence of particle morphology on the performance of composites is mainly attributed to the differences in localized stress–strain and electron conduction paths in the matrix. The previous work from the current team [100] demonstrated that spherical particles are more favorable to the transfer of thermal compare to hexagonal columnar particles, as illustrated in figure 8(d_3, d_4). Composites doped with spherical particles demonstrate improved thermal conductivity because the spherical particles enable a more uniform distribution of heat flow and reduce the accumulation of heat flow at sharp corners. At the present stage, there is a lack of targeted study on the influence of ceramic morphology on the thermophysical properties and electrical conductivity of metal matrix composites, and further exploration on this topic is still needed.

4.4. Interfacial bonding between ceramic particles and Cu matrix

In ceramic particles reinforced Cu matrix composites, the interface between ceramic particles and metal matrix is a bridge for particles to fully exert their reinforcing effect. Strong interfacial bonding is the key to the development of composites with excellent comprehensive performance [186–188]. The matrix/ceramic interface is generally divided into mechanical bonding and chemical bonding [189]. Compared to mechanical bonding, the chemical bonding is more critical for particle reinforced composites. The chemical bonding enables the atoms of the particles to contact the atoms of the matrix, which facilitates the exchange of electrons at the interfaces [190]. It is beneficial to weaken the interface effect on the scattering of electrons, thereby improving the thermal conductivity and electrical conductivity. However, the weak interface is prone to initiate cracks and then causes the component failure under loading, which more likely cause interface fracture, ceramic particles shedding and interface corrosion damage, thus weakening the strengthening effect of ceramic particles [191, 192]. Overall, improved bonding would increase heat transfer, electrical conductivity and facilitate load transfer between ceramic particles and Cu matrix. Synergistic enhancement of the Cu matrix with better network

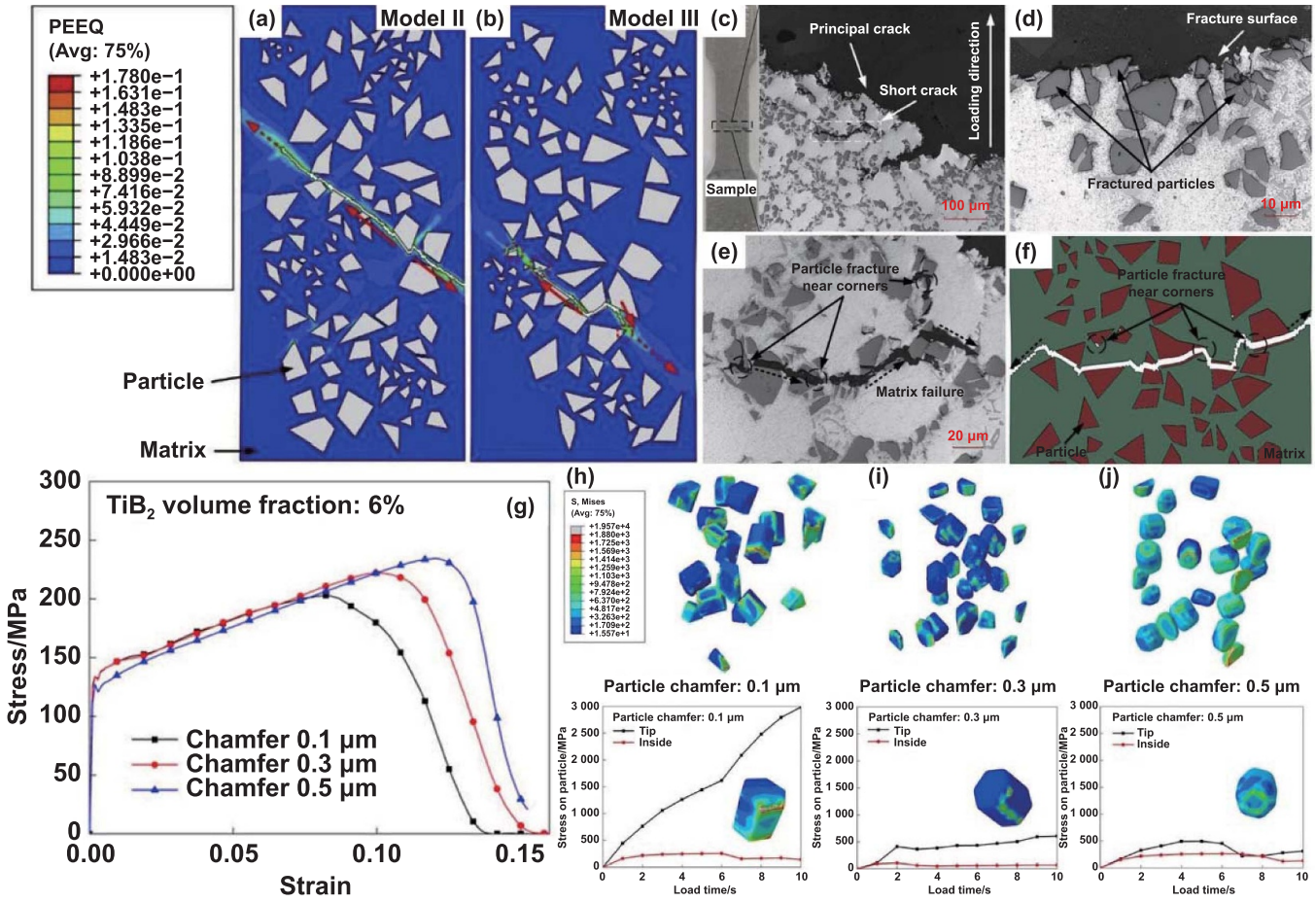

Figure 18. FEM results investigating the effect of particle morphology on the mechanical response of composites. (a), (b) The propagation of the matrix cracks for SiC/A359 composites. (c)–(e) Microscopic images of fracture surfaces for real specimens. (f) Simulated crack propagation. Reprinted from [151], Copyright (2019), with permission from Elsevier. (g) Simulated stress–strain curve of TiB_2/Cu composites with different particle chamfers. (h)–(j) Mises stress distribution on particles and the stress profiles of tip and inside of particle with different roundness. Reprinted from [170], Copyright (2022), with permission from Elsevier.

structure and stronger interfacial bonding is responsible for the improvement in composite properties [193, 194]. Zhang *et al* [195] pointed out that the enhanced interface bonding facilitates the reduction of CTE and improves dimensional stability of composites. The plastic deformation induced in the matrix around the interface is restrained by the reinforcement. When the interfacial bonding is stronger, the deformation is smaller, which is more favorable to limit the relaxation of residual stress.

Unfortunately, most ceramic particles have poor wettability with the Cu matrix and form a high contact angle, which results in weak interfacial bonding as illustrated in figures 19(a) and (b) [14, 196]. At the present stage, a variety of methods have been adopted to enhance the interfacial bonding between the ceramic phase and the Cu matrix, mainly including the surface metallization of ceramic and the matrix alloying. Furthermore, the *in-situ* synthesis of the ceramic phase in the matrix mentioned in section 2.4 is a more promising method to improve interfacial bonding. Tian *et al* [197] pretreated the surface of boron carbide (B_4C) particles by electroless Cu plating, and then mixed the Cu-coated B_4C with Cu-coated graphite to prepare a novel Cu-matrix self-lubricating composite. Compared with the composite reinforced by uncoated B_4C, Cu-coated B_4C reinforced Cu/graphite composite exhibit lower porosity, higher wear resistance and compressive strength owing to the improved wettability and interfacial bonding between the Cu-coated particles and matrix. Han *et al* [102] prepared reduced Cu-coated WC core–shell precursor powders by intermittent electrodeposition and SPS. This new preparation technique reduces the agglomeration of WC particles and enhances the interfacial bonding between the WC particles and the Cu matrix, which further improves the mechanical properties of the composite. Xiang *et al* [198] doped a small number of Ti element to optimize the interfacial bonding between the TiC and the Cu matrix and to enhance the strength of the composite. As shown in figures 19(c) and (d), the cracks propagate almost entirely along the edges of the TiC particles, and the Cu matrix does not show significant plastic deformation. This results from the poor bonding between TiC and

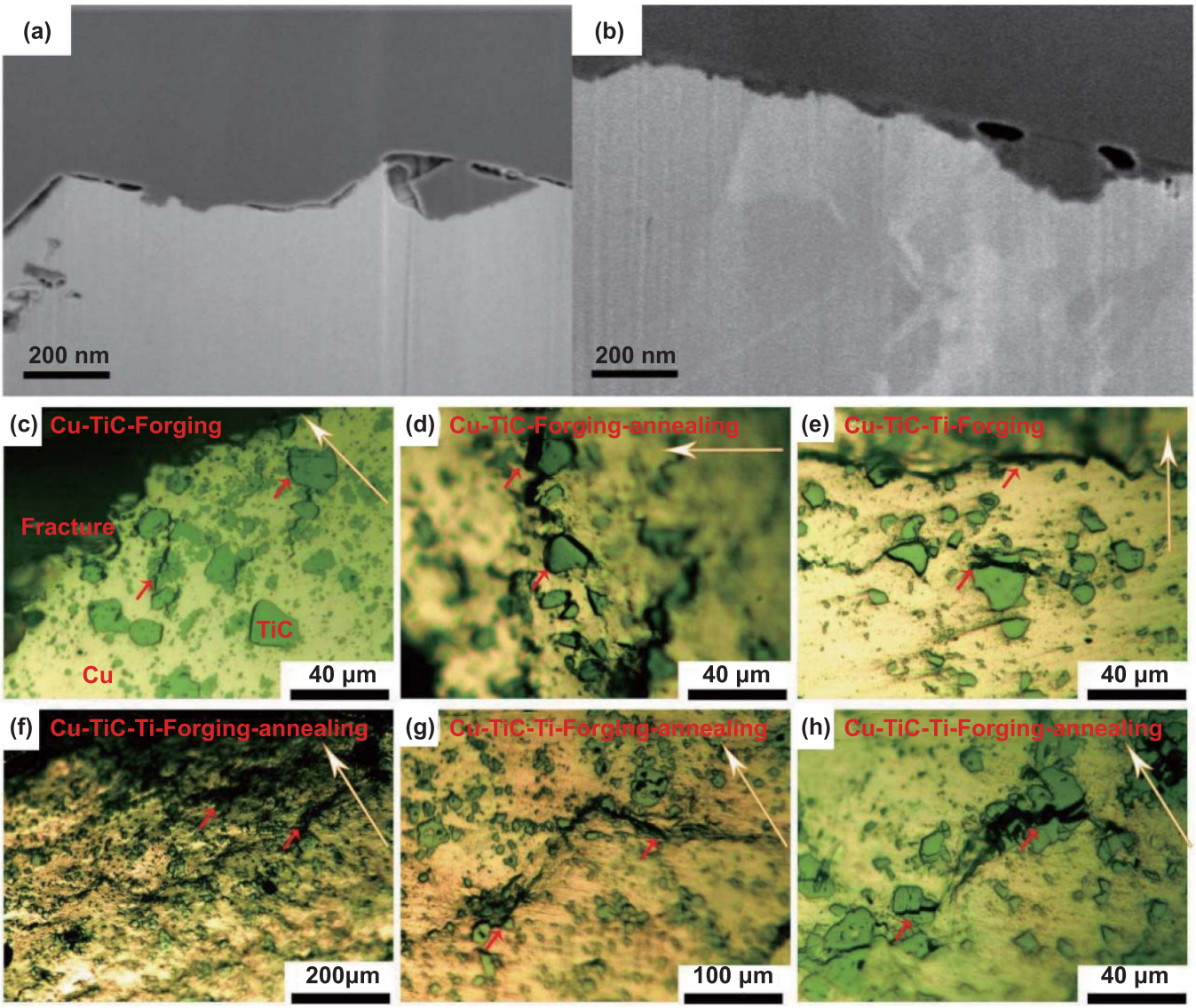

Figure 19. Interfacial bonding characteristics between ceramic particles and Cu matrix in composites. Differences between the interface microstructure of (a) uncoated and (b) coated SiC particles. Reprinted from [14], Copyright (2018), with permission from Elsevier. Optical microscopy images of the area around the cracks in: (c) forged 10%TiC/Cu; (d) forged 10%TiC/Cu annealed at 400 °C for 60 min; (e) forged 10%TiC/Cu-2%Ti; (f), (g) and (h) forged 10%TiC/Cu-2%Ti annealed at 400 °C for 60 min. Reprinted from [198], Copyright (2021), with permission from Elsevier.

the Cu matrix, which cannot achieve the load transfer process from the Cu matrix to the TiC particles. By contrast, for the forged 10%TiC/Cu-2%Ti samples, the interface between ceramic particles and the Cu matrix is significantly enhanced. Especially after annealing, the Cu matrix experiences significant plastic deformation and all the cracks appear within the Cu matrix or the TiC particles, suggesting an excellent interfacial bonding between the ceramic particles and the Cu matrix. During sintering process, Ti reacts with TiC particles to form non-stoichiometric TiC_x ($x < 1$). Meanwhile, TiC dissolves to form non-stoichiometric TiC_x and reprecipitates through the reaction of C and Ti during the succedent sintering process. Therefore, the conversion of stoichiometric TiC to non-stoichiometric TiC_x and the formation of non-stoichiometric TiC_x significantly enhance the bonding strength at the interfaces. This optimization of the interfacial bonding between the TiC particles and the Cu matrix enhances the strength and hardness of the composites by more than 40%.

5. Summary and prospect

Ceramic particles reinforced Cu matrix composites demonstrate excellent comprehensive performance by combining the high thermal conductivity and electrical conductivity of metallic Cu with the high specific strength and high temperature stability of the ceramic phase. Composites with low ceramic particle content (<5 wt.%) are beneficial for achieving the synergistic enhancement in strength and thermal and electrical conductivity to meet their requirements in electrical contact materials, heat transfer and conductive components, such as integrated circuit lead frame and brush. In comparison, the

high content of ceramic particle can greatly limit the thermal expansion behavior of the Cu matrix and enhance its strength and wear resistance, which makes the composites ideal electronic packaging materials. The current research is focusing on obtaining uniformly dispersed ceramic particles in the matrix and the rational design and control of the composite structure. Several preparation processes have developed in preparing ceramic particles reinforced Cu matrix composites and different preparation methods would directly determine the dispersion degree of ceramic particles in the matrix and its strengthening effect. This article reviews the advanced powder metallurgy processes including: mechanical alloying, spark plasma sintering, internal oxidation and *in-situ* method and analyzes each process according to its features and advantages. In fact, the Cu matrix composites fabricated by the various techniques tend to possess different comprehensive properties. The mechanical alloying and spark plasma sintering have a more prominent contribution to the improvement of grain refinement and densification of composite, as well as dispersion of particles. While the internal oxidation and *in-situ* method could greatly enhance the interfacial bonding between the ceramic phase and the metal matrix. These preparation processes can obtain satisfactory improvements of comprehensive performance compared to the conventional powder metallurgical processes. Furthermore, combining these advanced preparation techniques is beneficial to give full play to the advantages of various technologies while avoiding their disadvantages to further improve the comprehensive performance.

The introduction of fine ceramic particles in metal matrix could provide strong resistance to grain boundary migration and effectively hinder the motion of dislocations. The resulting grain refinement strengthening, dislocation strengthening, Orowan strengthening, and load transfer strengthening significantly improve the mechanical properties of the composites. The theoretical models of mechanical parameters, thermal expansion and thermal conductivity behavior have been successfully applied to the prediction and design of composites according to the nature and content of the metal and reinforcement. However, the non-uniform stress distribution, thermal residual stress, matrix plastic deformation and microstructure defects in the composites would also significantly affect its comprehensive performance. The improved models and FEM have been utilized to further understand the effect of the internal stress–strain behavior of composites by many researchers. On this basis, further development of the more applicable and comprehensive theoretical models and the FEM process is still the focus of future research.

In addition, the content, size, morphology of the ceramic particles and the interfacial bonding between ceramic phase and matrix will directly determine the final properties of the composites. Ceramic content is the dominant factor to regulate the strength and ductility of the Cu matrix composite. The size and morphology of ceramic particles can affect the stress accumulation and deformation inside the matrix as well as the conduction paths, resulting in changes in the properties of the composites. In general, the fine, uniformly dispersed and nearly spherical ceramic particles are more conducive to enhance the strength of composites and limit their thermal expansion behavior. By contrast, large-sized particles would reduce the hindrance of the ceramic to electrons, thereby improving the thermal and electrical conductivity of the composites. Cu matrix composites reinforced with angular particles exhibit higher yield strength and work hardening rate but slightly lower ductility and conductivity than those reinforced with spherical particles. Meanwhile, the stronger interfacial bonding can improve the heat transfer, electrical conductivity and load transfer between the ceramic phase and the Cu matrix owing to the synergistic enhancement of the Cu matrix with better network structure and stronger interfacial bonding between the two phases.

Overall, the research on ceramic reinforced Cu matrix composites keeps ongoing. How to further combine the advanced preparation processes and their advantages while avoiding the disadvantages of the various techniques is the focus of further studies. Besides, it is also the priorities of future research to mix high-performance CNTs and carbon fibers, etc, as well as advanced MAX-phase ceramic materials into Cu matrix composites. In the foreseeable future, more precise design and manipulation of composite microstructure, such as network structure and gradient structure, is expected to further improve its comprehensive properties and to meet the growing demand in the field of Cu matrix composites.

Acknowledgments

This work was supported by National Natural Science Foundation of China (No. 51971101), Science and Technology Development Program of Jilin Province, China (20230201146G X), and Exploration Foundation of State Key Laboratory of Automotive Simulation and Control (asclzytsxm-202015).

ORCID iDs

Feng Qiu https://orcid.org/0000-0003-4741-7906
Lai-Chang Zhang https://orcid.org/0000-0003-0661-2051

References

[1] Khdair A I and Ibrahim A 2022 Effect of graphene addition on the physicomechanical and tribological properties of Cu nanocomposites *Int. J. Miner. Metall. Mater.* **29** 161–7
[2] Abd-Elwahed M S, Wagih A and Najjar I M R 2020 Correlation between micro/nano-structure, mechanical and tribological properties of copper-zirconia nanocomposites *Ceram. Int.* **46** 56–65
[3] Pratik A, Biswal S K and Haridoss P 2020 Impact of enhanced interfacial strength on physical, mechanical and tribological properties of copper/reduced graphene oxide composites: microstructural investigation *Ceram. Int.* **46** 22539–49
[4] Qin Y Q, Tian Y, Peng Y Q, Luo L M, Zan X, Xu Q and Wu Y C 2020 Research status and development trend of preparation technology of ceramic particle dispersion strengthened copper-matrix composites *J. Alloys Compd.* **848** 156475

[5] Zhou G H and Ding H Y 2013 Wear performance of alumina-reinforced copper-matrix composites prepared by powder metallurgy *Proc. Inst. Mech. Eng. J.* **227** 1011–7

[6] Zhan Y Z and Zhang G D 2022 Elevated temperature friction and wear behavior of SiC-reinforced copper matrix composites *Int. J. Mater. Res.* **95** 1040–5

[7] Pan J M, Yin J W, Xia Y F, Yao D X, Liang H Q, Zuo K H and Zeng Y P 2019 The microstructure and properties of bronze matrix composites with surface-modified graphite by titanium carbide adhesion *Tribol. Int.* **140** 105892

[8] Shaik M A and Golla B R 2020 Mechanical, tribological and electrical properties of ZrB_2 reinforced Cu processed via milling and high-pressure hot pressing *Ceram. Int.* **46** 20226–35

[9] Moustafa E B and Taha M A 2021 Evaluation of the microstructure, thermal and mechanical properties of Cu/SiC nanocomposites fabricated by mechanical alloying *Int. J. Miner. Metall. Mater.* **28** 475–86

[10] Zhang P C, Jie J C, Gao Y, Li H, Cao Z Q, Wang T M and Li T J 2015 Preparation and properties of TiB_2 particles reinforced Cu-Cr matrix composite *Mater. Sci. Eng.* A **642** 398–405

[11] Feng J, Song K X, Liang S H, Guo X H and Li S L 2022 Mechanical properties and electrical conductivity of oriented-SiC-whisker-reinforced Al_2O_3/Cu composites *J. Mater. Res. Technol.* **20** 1470–80

[12] Zhao J, Wang X W, Shu F Y, Jiang S S, Ma P, Zhao Y X and Yu Z S 2020 Research on microstructure of copper coatings on AlN ceramic surface by laser cladding and brazing *Mater. Res. Express* **7** 075104

[13] Li F P, Wang W X, Dang W, Zhao K and Tang Y F 2020 Wetting mechanism and bending property of Cu/Al_2O_3 laminated composites with pretreated CuO interlayer *Ceram. Int.* **46** 17392–9

[14] Jarząbek D M, Dziekoński C, Dera W, Chrzanowska J and Wojciechowski T 2018 Influence of Cu coating of SiC particles on mechanical properties of Ni/SiC co-electrodeposited composites *Ceram. Int.* **44** 21750–8

[15] Nalepka K, Sztwiertnia K and Nalepka P 2016 Preferred orientation relationships at the Cu/α-Al_2O_3 interface: identification and theoretical explanation *Acta Mater.* **104** 156–65

[16] Mu Z, Geng H R, Li M M, Nie G L and Leng J F 2013 Effects of Y_2O_3 on the property of copper based contact materials *Composites* B **52** 51–55

[17] Han T L, Hou C, Zhao Z, Huang X T, Tang F W, Li Y R and Song X Y 2022 W–Cu composites with excellent comprehensive properties *Composites* B **233** 109664

[18] Luo X, Yang Y Q, Mei Y W, Huang B, Yuan M N and Chen Y 2007 Titanium interlayers as adhesion promoters for SiC_f/Cu composites *Scr. Mater.* **56** 569–72

[19] Şap S, Turgut A and Uzun M 2021 Investigation of microstructure and mechanical properties of Cu/Ti–B–SiC_p hybrid composites *Ceram. Int.* **47** 29919–29

[20] Güler O, Varol T, Alver Ü and Canakci A 2020 Effect of Al_2O_3 content and milling time on the properties of silver coated Cu matrix composites fabricated by electroless plating and hot pressing *Mater. Today Commun.* **24** 101153

[21] Zhang C C, Zhang J, Luo G Q, Liu Y, Shen Q and Zhang L M 2018 Preparation and properties of W-SiC/Cu composites by tape casting and hot-pressing sintering *Mater. Sci. Technol.* **34** 1353–61

[22] Avettand-Fènoël M-N, Simar A, Shabadi R, Taillard R and de Meester B 2014 Characterization of oxide dispersion strengthened copper based materials developed by friction stir processing *Mater. Des.* **60** 343–57

[23] Barmouz M, Asadi P, Besharati Givi M K and Taherishargh M 2011 Investigation of mechanical properties of Cu/SiC composite fabricated by FSP: effect of SiC particles' size and volume fraction *Mater. Sci. Eng.* A **528** 1740–9

[24] Khosroshahi R A, Nemati N, Emamy M, Parvini N and Zolriasatein A 2012 Investigation of wear properties of Al-4.5wt.%Cu nano-composite reinforced with different weight percent of TiC nano particles produced by mechanical alloying *Adv. Mater. Res.* **545** 124–8

[25] Zhang J, He L F and Zhou Y C 2009 Highly conductive and strengthened copper matrix composite reinforced by $Zr_2Al_3C_4$ particulates *Scr. Mater.* **60** 976–9

[26] Prosviryakov A S 2015 SiC content effect on the properties of Cu-SiC composites produced by mechanical alloying *J. Alloys Compd.* **632** 707–10

[27] Lian W Q, Mai Y, Wang J, Zhang L Y, Liu C S and Jie X H 2019 Fabrication of graphene oxide-Ti_3AlC_2 synergistically reinforced copper matrix composites with enhanced tribological performance *Ceram. Int.* **45** 18592–8

[28] Wang X L, Wang Y P, Su Y and Qu Z G 2019 Synergetic strengthening effects on copper matrix induced by Al_2O_3 particle revealed from micro-scale mechanical deformation and microstructure evolutions *Ceram. Int.* **45** 14889–95

[29] Saheb N, Iqbal Z, Khalil A, Hakeem A S, Al Aqeeli N, Laoui T, Al-Qutub A and Kirchner R 2012 Spark plasma sintering of metals and metal matrix nanocomposites: a review *J. Nanomater.* **2012** 983470

[30] Li C G, Xie Y H, Zhou D S, Zeng W, Wang J, Liang J M and Zhang D L 2019 A novel way for fabricating ultrafine grained Cu-4.5 vol% Al_2O_3 composite with high strength and electrical conductivity *Mater. Charact.* **155** 109775

[31] Hosseini Vajargah P, Abdizadeh H and Baghchesara M A 2015 Fabrication of TiB_2 nanoparticulates-reinforced aluminum matrix composites by powder metallurgy route *J. Compos. Mater.* **49** 3115–25

[32] Baghani M and Aliofkhazraei M 2017 CuCrW(Al_2O_3) nanocomposite: mechanical alloying, microstructure, and tribological properties *Int. J. Miner. Metall. Mater.* **24** 1321–34

[33] Aghamiri S M S, Oono N, Ukai S, Kasada R, Noto H, Hishinuma Y and Muroga T 2018 Microstructure and mechanical properties of mechanically alloyed ODS copper alloy for fusion material application *Nucl. Mater. Energy* **15** 17–22

[34] Bera S and Manna I 2012 Synthesis of CuCr and CuCrAg alloy with nano-ceramic dispersion by mechanical alloying and consolidation by laser assisted sintering *Mater. Chem. Phys.* **132** 109–18

[35] Ni J J, Li J, Luo W, Han Q, Yin Y B, Jia Z F, Huang B X, Hu C C and Xu Z L 2018 Microstructure and properties of *in-situ* TiC reinforced copper nanocomposites fabricated via long-term ball milling and hot pressing *J. Alloys Compd.* **755** 24–28

[36] Khamaj A, Farouk W M, Shewakh W M, Abu-Oqail A M I, Wagih A and Abu-Okail M 2021 Effect of lattice structure evolution on the thermal and mechanical properties of Cu–Al_2O_3/GNPs nanocomposites *Ceram. Int.* **47** 16511–20

[37] Zawrah M F, Abdel-Kader H and Elbaly N E 2012 Fabrication of Al_2O_3-20vol.% Al nanocomposite powders using high energy milling and their sinterability *Mater. Res. Bull.* **47** 655–61

[38] Fogagnolo J B, Velasco F, Robert M H and Torralba J M 2003 Effect of mechanical alloying on the morphology, microstructure and properties of aluminium matrix composite powders *Mater. Sci. Eng.* A **342** 131–43

[39] Zawrah M F, Zayed H A, Essawy R A, Nassar A H and Taha M A 2013 Preparation by mechanical alloying, characterization and sintering of Cu-20wt.% Al_2O_3 nanocomposites *Mater. Des.* **46** 485–90

[40] Taha M A and Zawrah M F 2017 Effect of nano ZrO_2 on strengthening and electrical properties of Cu-matrix nanocomposits prepared by mechanical alloying *Ceram. Int.* **43** 12698–704

[41] Akbarpour M R, Salahi E, Alikhani Hesari F, Simchi A and Kim H S 2014 Microstructure and compressibility of SiC nanoparticles reinforced Cu nanocomposite powders processed by high energy mechanical milling *Ceram. Int.* **40** 951–60

[42] Zebarjad S M and Sajjadi S A 2007 Dependency of physical and mechanical properties of mechanical alloyed Al–Al_2O_3 composite on milling time *Mater. Des.* **28** 2113–20

[43] Wang F L, Li Y P, Yamanaka K, Wakon K, Harata K and Chiba A 2014 Influence of two-step ball-milling condition on electrical and mechanical properties of TiC-dispersion-strengthened Cu alloys *Mater. Des.* **64** 441–9

[44] Huang F, Wang H, Yang B, Liao T and Wang Z Y 2019 Uniformly dispersed Y_2O_3 nanoparticles in nanocrystalline copper matrix via multi-step ball milling and reduction process *Mater. Lett.* **242** 119–22

[45] Shao Z Y, Sun Y, Liu W X, Zhang X Q and Jiang X S 2016 Effects of multi-phase reinforcements on microstructures, mechanical and tribological properties of Cu/Ti_3SiC_2/C/BN/GNPs nanocomposites sintered by vacuum hot-pressing and hot isostatic pressing *Metals* **6** 324

[46] Jiang X S, Liu W X, Li Y J, Shao Z Y, Luo Z P, Zhu D G and Zhu M H 2018 Microstructures and mechanical properties of Cu/Ti_3SiC_2/C/graphene nanocomposites prepared by vacuum hot-pressing sintering and hot isostatic pressing *Composites* B **141** 203–13

[47] Kelly J P and Graeve O A 2015 Spark plasma sintering as an approach to manufacture bulk materials: feasibility and cost savings *JOM* **67** 29–33

[48] Oliver U C, Sunday A V, Christain E I E I and Elizabeth M M 2021 Spark plasma sintering of aluminium composites—a review *Int. J. Adv. Manuf. Technol.* **112** 1819–39

[49] Munir Z A and Ohyanagi M 2021 Perspectives on the spark plasma sintering process *J. Mater. Sci.* **56** 1–15

[50] Nisar A, Zhang C, Boesl B and Agarwal A 2021 Unconventional materials processing using spark plasma sintering *Ceramics* **4** 20–39

[51] Zhang Z H, Liu Z F, Lu J F, Shen X B, Wang F C and Wang Y D 2014 The sintering mechanism in spark plasma sintering—proof of the occurrence of spark discharge *Scr. Mater.* **81** 56–59

[52] Naghikhani M, Ardestani M and Moazami-Goudarzi M 2021 Microstructure, mechanical properties and wear performance of WC/brass composites produced by pressureless and spark plasma sintering processes *Met. Mater. Int.* **27** 1639–48

[53] Qin Y Q, Zhuang Y, Wang Y, Zhang Y F, Luo L M, Zan X and Wu Y C 2022 Enhanced mechanical and electrical properties of CuCrZr-WC alloy prepared by mechanical alloying and spark plasma sintering *Fusion Eng. Des.* **180** 113166

[54] Sovizi S and Seraji M E 2019 The densification behavior of metals and alloys during spark plasma sintering: a mini-review *Sci. Sinter.* **51** 135–52

[55] Saheb N, Hayat U and Hassan S F 2019 Recent advances and future prospects in spark plasma sintered alumina hybrid nanocomposites *Nanomaterials* **9** 1607

[56] Venkatesh V S S and Deoghare A B 2022 Effect of sintering mechanisms on the mechanical behaviour of SiC and kaoline reinforced hybrid aluminium metal matrix composite fabricated through powder metallurgy technique *Silicon* **14** 5481–93

[57] Dash K, Ray B C and Chaira D 2012 Synthesis and characterization of copper-alumina metal matrix composite by conventional and spark plasma sintering *J. Alloys Compd.* **516** 78–84

[58] Senthilnathan N, Annamalai A R and Venkatachalam G 2018 Microstructure and mechanical properties of spark plasma sintered tungsten heavy alloys *Mater. Sci. Eng.* A **710** 66–73

[59] Akbarpour M R, Mousa Mirabad H, Khalili Azar M, Kakaei K and Kim H S 2020 Synergistic role of carbon nanotube and SiC_n reinforcements on mechanical properties and corrosion behavior of Cu-based nanocomposite developed by flake powder metallurgy and spark plasma sintering process *Mater. Sci. Eng.* A **786** 139395

[60] Zhou D S, Wang X K, Muránsky O, Wang X R, Xie Y H, Yang C and Zhang D L 2018 Heterogeneous microstructure of an Al_2O_3 dispersion strengthened Cu by spark plasma sintering and extrusion and its effect on tensile properties and electrical conductivity *Mater. Sci. Eng.* A **730** 328–35

[61] Shi X L, Yang H and Wang S 2009 Spark plasma sintering of W-15Cu alloy from ultrafine composite powder prepared by spray drying and calcining-continuous reduction technology *Mater. Charact.* **60** 133–7

[62] Seyyedi A and Abdoos H 2022 An examination of microstructure and dry wear properties of nano-Y_2O_3 incorporated in fine-grained W-Ni-Cu alloy prepared by conventional and spark plasma sintering *Int. J. Refract. Met. Hard Mater.* **102** 105728

[63] Bahador A, Umeda J, Hamzah E, Yusof F, Li X C and Kondoh K 2020 Synergistic strengthening mechanisms of copper matrix composites with TiO_2 nanoparticles *Mater. Sci. Eng.* A **772** 138797

[64] Li K W and Gao F 2018 Heterogeneity of grain refinement and texture formation during pulsed electric current sintering of conductive powder: a case study in copper powder *Adv. Powder Technol.* **29** 3385–93

[65] Pan Y, Xiao S Q, Lu X, Zhou C, Li Y, Liu Z W, Liu B W, Xu W, Jia C C and Qu X H 2019 Fabrication, mechanical properties and electrical conductivity of Al_2O_3 reinforced Cu/CNTs composites *J. Alloys Compd.* **782** 1015–23

[66] Chmielewski M, Pietrzak K, Strojny-Nędza A, Jarzabek D and Nosewicz S 2017 Investigations of interface properties in copper-silicon carbide composites *Arch. Metall. Mater.* **62** 1315–8

[67] Wang Q C, Chen M H, Shan Z M, Sui C, Zhang L, Zhu S L and Wang F H 2017 Comparative study of mechanical and wear behavior of Cu/WS_2 composites fabricated by spark plasma sintering and hot pressing *J. Mater. Sci. Technol.* **33** 1416–23

[68] Zhou X Y, Hu Z and Yi D Q 2019 Enhancing the oxidation resistance and electrical conductivity of alumina reinforced copper-based composites via introducing Ag and annealing treatment *J. Alloys Compd.* **787** 786–93

[69] Liu X Y *et al* 2022 Effect of chromium interlayer thickness on interfacial thermal conductance across copper/diamond interface *Int. J. Miner. Metall. Mater.* **29** 2020–31

[70] Dong Y, Wang X K, Xie Y H, Yang C and Zhou D S 2020 Tunable microstructures and tensile mechanical properties of oxide-dispersion-strengthened Cu by extrusion and secondary processing *J. Alloys Compd.* **812** 152112

[71] Zheng R G and Li N N 2019 Mechanical properties and electrical conductivity of nano-La_2O_3 reinforced copper matrix composites fabricated by spark plasma sintering *Mater. Res. Express* **6** 106527

[72] Rajkovic V, Bozic D and Jovanovic M T 2010 Effects of copper and Al_2O_3 particles on characteristics of Cu-Al_2O_3 composites *Mater. Des.* **31** 1962–70

[73] Zhang X H, Li X X, Chen H, Li T B, Su W and Guo S D 2016 Investigation on microstructure and properties of Cu-Al_2O_3 composites fabricated by a novel *in-situ* reactive synthesis *Mater. Des.* **92** 58–63

[74] Yan Z Q, Chen F, Ye F X, Zhang D P and Cai Y X 2016 Microstructures and properties of Al_2O_3 dispersion-strengthened copper alloys prepared through different methods *Int. J. Miner. Metall. Mater.* **23** 1437–43

[75] Xiang Z Q, Li Z, Lei Q, Xiao Z and Pang Y 2015 High temperature mechanical behavior of alumina dispersion strengthened copper alloy with high content of alumina *Trans. Nonferrous Met. Soc. China* **25** 444–50

[76] Zhao Z Q, Xiao Z, Li Z, Zhu M N and Yang Z Q 2017 Characterization of dispersion strengthened copper alloy prepared by internal oxidation combined with mechanical alloying *J. Mater. Eng. Perform.* **26** 5641–7

[77] Zhao S X, Zhang T X and Wang M J 2022 Factors affecting the coarsening and agglomeration of alumina particles in Cu–Al_2O_3 composites prepared with internal oxidation *Adv. Eng. Mater.* **24** 2101169

[78] Han S Z, Joh H, Ahn J H, Lee J, Kim S M, Lim S H and Son Y G 2015 Ti-added alumina dispersion-strengthened Cu alloy fabricated by oxidation *J. Alloys Compd.* **622** 384–7

[79] Zhou X Y, Yi D Q, Nyborg L, Hu Z, Huang J and Cao Y 2017 Influence of Ag addition on the microstructure and properties of copper-alumina composites prepared by internal oxidation *J. Alloys Compd.* **722** 962–9

[80] Long F, Guo X H, Song K X, Liu J Q, Wang X, Yang Y B and Li S L 2022 An internal-oxidation-based strategy induced high-density alumina *in-situ* nanoprecipitation and carbon nanotube interface optimization for co-reinforcing copper matrix composites *Composites* B **229** 109455

[81] Xu K, Chen X H, Zhou H L, Bi L M, Fu S L, Li W, Liu X K, Ma F C, Zhang K and Liu P 2019 Preparation and formation mechanism of CNTs/Cu-Al_2O_3 composite powders by *in situ* CVD using internally-oxidized Cu-Al alloy powders *Mater. Lett.* **254** 390–3

[82] Guo X, Chen X H, Liu P, Zhou H L, Fu S L, Li W, Liu X K, Ma F C and Wu Z P 2021 Preparation and mechanical properties of copper matrix composites reinforced by carbon nanotubes and Al_2O_3 *Adv. Eng. Mater.* **23** 2001490

[83] Jiang Y H, Wang C, Liang S H, Ren J Q, Du X and Liu F 2016 TiB_2 (-TiB)/Cu *in-situ* composites prepared by hot-press with the sintering temperature just beneath the melting point of copper *Mater. Charact.* **121** 76–81

[84] Zhang D D, He X Y, Zhao H and Gao Y L 2022 Properties of TiC_p/Cu composites fabricated by powder metallurgy and electrodeless copper plating *Mater. Sci. Technol.* **38** 5–11

[85] Fathy A 2018 Investigation on microstructure and properties of Cu-ZrO_2 nanocomposites synthesized by *in situ* processing *Mater. Lett.* **213** 95–99

[86] Xie K, Han C, Liu J and Tan Y L 2020 Fabrication of Cu-ZrO_2 composites by *in situ* oxidation of liquid Cu–Zr alloy *J. Nanoparticle Res.* **22** 80

[87] Dong Z, Hu W Q, Ma Z Q, Li C and Liu Y C 2019 The synthesis of composite powder precursors *via* chemical processes for the sintering of oxide dispersion-strengthened alloys *Mater. Chem. Front.* **3** 1952–72

[88] Zhang S R, Kang H J, Li R G, Zou C L, Guo E Y, Chen Z N and Wang T M 2019 Microstructure evolution, electrical conductivity and mechanical properties of dual-scale Cu_5Zr/ZrB_2 particulate reinforced copper matrix composites *Mater. Sci. Eng.* A **762** 138108

[89] Pan S H, Zheng T Q, Yao G C, Chi Y T, De Rosa I and Li X C 2022 High-strength and high-conductivity *in situ* Cu–TiB_2 nanocomposites *Mater. Sci. Eng.* A **831** 141952

[90] Sobhani M, Mirhabibi A, Arabi H and Brydson R M D 2013 Effects of *in situ* formation of TiB_2 particles on age hardening behavior of Cu-1wt% Ti-1wt% TiB_2 *Mater. Sci. Eng.* A **577** 16–22

[91] Tjong S C and Ma Z Y 2000 Microstructural and mechanical characteristics of *in situ* metal matrix composites *Mater. Sci. Eng.* R **29** 49–113

[92] Tun K S and Gupta M 2007 Improving mechanical properties of magnesium using nano-yttria reinforcement and microwave assisted powder metallurgy method *Compos. Sci. Technol.* **67** 2657–64

[93] Garcés G, Rodríguez M, Pérez P and Adeva P 2007 High temperature mechanical properties of Mg-Y_2O_3 composite: competition between texture and reinforcement contributions *Compos. Sci. Technol.* **67** 632–7

[94] Zhuo H O, Tang J C and Ye N 2013 A novel approach for strengthening Cu-Y_2O_3 composites by *in situ* reaction at liquidus temperature *Mater. Sci. Eng.* A **584** 1–6

[95] Yu Z L, Zhu H G, Huang J W, Li J L and Xie Z H 2017 Processing and characterization of *in-situ* ultrafine TiB_2-Cu composites from Ti-B-Cu system *Powder Technol.* **320** 66–72

[96] Ding H M, Liu Q, Wang X L, Fan X L, Krzystyniak M, Glandut N and Li C 2018 Effects of boron addition on the microstructure and properties of *in situ* synthesis TiC reinforced Cu–Ti–C composites *J. Alloys Compd.* **766** 66–73

[97] Guo S Y, Zhang X, Shi C S, Liu E Z, He C N, He F and Zhao N Q 2019 Enhanced mechanical properties and electrical conductivity of graphene nanoplatelets/Cu composites by *in situ* formation of Mo_2C nanoparticles *Mater. Sci. Eng.* A **766** 138365

[98] Zhang D D, Bai F, Sun L P, Wang Y and Wang J 2017 Compression properties and electrical conductivity of *in-situ* 20 vol.% nano-sized TiC_x/Cu composites with different particle size and morphology *Materials* **10** 499

[99] Sadeghi N, Aghajani H and Akbarpour M R 2018 Microstructure and tribological properties of *in-situ* TiC-C/Cu nanocomposites synthesized using different carbon sources (graphite, carbon nanotube and graphene) in the Cu-Ti-C system *Ceram. Int.* **44** 22059–67

[100] Yan Y F, Kou S Q, Yang H Y, Shu S L and Lu J B 2022 Effect mechanism of mono-particles or hybrid-particles on the thermophysical characteristics and mechanical properties of Cu matrix composites *Ceram. Int.* **48** 23033–43

[101] Zhou D S, Zhang D L, Kong C and Munroe P 2013 Factors controlling the tensile properties of ultrafine structured Cu-5vol%Al_2O_3 nanocomposite prepared by high energy mechanical milling and powder compact extrusion *Mater. Sci. Eng.* A **584** 67–72

[102] Han L, Wang J, Chen Y Y, Huang Y, Liu Y C and Wang Z M 2021 Fabrication and mechanical properties of WC nanoparticle dispersion-strengthened copper *Mater. Sci. Eng.* A **817** 141274

[103] Bazarnik P, Nosewicz S, Romelczyk-Baishya B, Chmielewski M, Strojny Nędza A, Maj J, Huang Y, Lewandowska M and Langdon T G 2019 Effect of spark plasma sintering and high-pressure torsion on the microstructural and mechanical properties of a Cu–SiC composite *Mater. Sci. Eng.* A **766** 138350

[104] Yan Y X, Zou J M, Zhang X H, Xiao Q, Chen B Q, Huang F, Li X X, Yang B and Liang T X 2021 Investigation on microstructure and properties of $TiC_{0.5}$-Al_2O_3/Cu composites fabricated by a novel *in-situ* reactive synthesis *Ceram. Int.* **47** 18858–65

[105] Wang S, Xie M, Zhang J M and Chen Y T 2014 Synthesis and properties of 0.3%Y_2O_3/0.3%La_2O_3/0.3%Al_2O_3/Cu composite *Sci. Eng. Compos. Mater.* **21** 517–20

[106] Tian B H, Liu P, Song K X, Li Y, Liu Y, Ren F Z and Su J H 2006 Microstructure and properties at elevated temperature of a nano-Al_2O_3 particles dispersion-strengthened copper base composite *Mater. Sci. Eng.* A **435–436** 705–10

[107] Lu J B, Shu S L, Qiu F, Wang Y W and Jiang Q C 2012 Compression properties and abrasive wear behavior of high volume fraction TiC_x-TiB_2/Cu composites fabricated by combustion synthesis and hot press consolidation *Mater. Des.* **40** 157–62

[108] Li T J, Wang Y Q, Yang M, Hou H L and Wu S J 2021 High strength and conductivity copper/graphene composites prepared by severe plastic deformation of graphene coated copper powder *Mater. Sci. Eng.* A **826** 141983

[109] Gao S, Nan Z L, Li Y, Zhao N, Liu Q Q, Xu G F, Cheng X N and Yang J 2020 Copper matrix thermal conductive composites with low thermal expansion for electronic packaging *Ceram. Int.* **46** 18019–25

[110] Cho S, Kikuchi K and Kawasaki A 2012 On the role of amorphous intergranular and interfacial layers in the thermal conductivity of a multi-walled carbon nanotube-copper matrix composite *Acta Mater.* **60** 726–36

[111] Wang Y P, Fu R D, Li Y J and Zhao L 2019 A high strength and high electrical conductivity Cu-Cr-Zr alloy fabricated by cryogenic friction stir processing and subsequent annealing treatment *Mater. Sci. Eng.* A **755** 166–9

[112] Li Y P, Xiao Z, Li Z, Zhou Z Y, Yang Z Q and Lei Q 2017 Microstructure and properties of a novel Cu-Mg-Ca alloy with high strength and high electrical conductivity *J. Alloys Compd.* **723** 1162–70

[113] Dong Q Y, Shen L N, Cao F, Jia Y L, Liao K J and Wang M P 2015 Effect of thermomechanical processing on the microstructure and properties of a Cu-Fe-P alloy *J. Mater. Eng. Perform.* **24** 1531–9

[114] Wang W, Guo E Y, Chen Z N, Kang H J, Chen Z J, Zou C L, Li R G, Yin G M and Wang T M 2018 Correlation between microstructures and mechanical properties of cryorolled CuNiSi alloys with Cr and Zr alloying *Mater. Charact.* **144** 532–46

[115] Li R G, Guo E Y, Chen Z N, Kang H J, Wang W, Zou C L, Li T J and Wang T M 2019 Optimization of the balance between high strength and high electrical conductivity in CuCrZr alloys through two-step cryorolling and aging *J. Alloys Compd.* **771** 1044–51

[116] Kulczyk M, Pachla W, Godek J, Smalc-Koziorowska J, Skiba J, Przybysz S, Wróblewska M and Przybysz M 2018 Improved compromise between the electrical conductivity and hardness of the thermo-mechanically treated CuCrZr alloy *Mater. Sci. Eng.* A **724** 45–52

[117] Edwards D J, Singh B N and Tähtinen S 2007 Effect of heat treatments on precipitate microstructure and mechanical properties of a CuCrZr alloy *J. Nucl. Mater.* **367–370** 904–9

[118] Vinogradov A, Patlan V, Suzuki Y, Kitagawa K and Kopylov V I 2002 Structure and properties of ultra-fine grain Cu-Cr-Zr alloy produced by equal-channel angular pressing *Acta Mater.* **50** 1639–51

[119] Yan Z Y, Ma Z, Liu L, Zhu S Z and Gao L H 2014 The ablation behavior of ZrB_2/Cu composite irradiated by high-intensity continuous laser *J. Eur. Ceram. Soc.* **34** 2203–9

[120] Yin J W, Zhou P L, Liang H Q, Yao D X, Xia Y F, Zuo K H and Zeng Y P 2020 Microstructure and mechanical properties of Cu matrix composites reinforced by TiB_2/TiN ceramic reinforcements *Acta Metall. Sin.* **33** 1609–17

[121] Dong B X, Li Q, Wang Z F, Liu T S, Yang H Y, Shu S L, Chen L Y, Qiu F, Jiang Q C and Zhang L C 2021 Enhancing strength-ductility synergy and mechanisms of Al-based composites by size-tunable *in-situ* TiB_2 particles with specific spatial distribution *Composites* B **217** 108912

[122] Fathy A and El-Kady O 2013 Thermal expansion and thermal conductivity characteristics of Cu-Al_2O_3 nanocomposites *Mater. Des.* **46** 355–9

[123] Xu J Z, Gao B Z and Kang F Y 2016 A reconstruction of Maxwell model for effective thermal conductivity of composite materials *Appl. Therm. Eng.* **102** 972–9

[124] Ghosh G, Miyake J and Fine M E 1997 The systems-based design of high-strength, high-conductivity alloys *JOM* **49** 56–60

[125] Zhang L, Qu X H, He X B, Duan B H, Ren S B and Qin M L 2008 Thermo-physical and mechanical properties of high volume fraction SiC_p/Cu composites prepared by pressureless infiltration *Mater. Sci. Eng.* A **489** 285–93

[126] Qin Y Q, Tian Y, Zhuang Y, Luo L M, Zan X and Wu Y C 2021 Effects of solid–liquid doping and spark plasma sintering on the microstructure and mechanical properties of Y_2O_3-doped copper matrix composites *Vacuum* **192** 110436

[127] Mallik S, Ekere N, Best C and Bhatti R 2011 Investigation of thermal management materials for automotive electronic control units *Appl. Therm. Eng.* **31** 355–62

[128] Zweben C 1992 Metal-matrix composites for electronic packaging *JOM* **44** 15–23

[129] Zeng J, Peng C Q, Wang R C and Wang X F 2015 Research and development of metal matrix composites for electronic packaging *Chin. J. Nonferr. Met.* **25** 3255–70

[130] Hashin Z and Shtrikman S 1963 A variational approach to the theory of the elastic behaviour of multiphase materials *J. Mech. Phys. Solids* **11** 127–40

[131] Affdl J C H and Kardos J L 1976 The Halpin-Tsai equations: a review *Polym. Eng. Sci.* **16** 344–52

[132] Li Y, Zhao Y H, Ortalan V, Liu W, Zhang Z H, Vogt R G, Browning N D, Lavernia E J and Schoenung J M 2009 Investigation of aluminum-based nanocomposites with ultra-high strength *Mater. Sci. Eng.* A **527** 305–16

[133] Sekine H and Chent R 1995 A combined microstructure strengthening analysis of SiC_p/Al metal matrix composites *Composites* **26** 183–8

[134] Wang M L, Chen D, Chen Z, Wu Y, Wang F F, Ma N H and Wang H W 2014 Mechanical properties of *in-situ* TiB_2/A356 composites *Mater. Sci. Eng.* A **590** 246–54

[135] Kim C S, Sohn I, Nezafati M, Ferguson J B, Schultz B F, Bajestani-Gohari Z, Rohatgi P K and Cho K 2013 Prediction models for the yield strength of particle-reinforced unimodal pure magnesium (Mg) metal matrix nanocomposites (MMNCs) *J. Mater. Sci.* **48** 4191–204

[136] Sanaty-Zadeh A 2012 Comparison between current models for the strength of particulate-reinforced metal matrix nanocomposites with emphasis on consideration of Hall-Petch effect *Mater. Sci. Eng.* A **531** 112–8

[137] Gao Y L, Kou S Q, Dai J N, Wang Z F, Shu S L, Zhang S, Qiu F and Jiang Q C 2021 Microstructural configuration and compressive deformation behavior of a TiAl composite reinforced by Mn and *in situ* Ti_2AlC particles *Mater. Sci. Eng.* A **823** 141772

[138] Li Q, Qiu F, Gao Y Y, Dong B X, Shu S L, Lv M M, Yang H Y, Zhao Q L and Jiang Q C 2019 Microstructure refinement and strengthening mechanisms of bimodal-sized and dual-phased (TiC_n-Al_3Ti_m)/Al hybrid composites assisted ultrasonic vibration *J. Alloys Compd.* **788** 1309–21

[139] Mirza F A and Chen D L 2012 An analytical model for predicting the yield strength of particulate-reinforced

metal matrix nanocomposites with consideration of porosity *Nanosci. Nanotechnol. Lett.* **4** 794–800
[140] Bhat A, Balla V K, Bysakh S, Basu D, Bose S and Bandyopadhyay A 2011 Carbon nanotube reinforced Cu-10Sn alloy composites: mechanical and thermal properties *Mater. Sci. Eng.* A **528** 6727–32
[141] Geng R, Qiu F and Jiang Q C 2018 Reinforcement in Al matrix composites: a review of strengthening behavior of nano-sized particles *Adv. Eng. Mater.* **20** 1701089
[142] Hull D and Bacon D J 2011 Origin and multiplication of dislocations *Introduction to Dislocations* 5th edn, ed D Hull and D J Bacon (Amsterdam: Elsevier) pp 157–69
[143] Shu K M and Tu G C 2003 The microstructure and the thermal expansion characteristics of Cu/SiC_p composites *Mater. Sci. Eng.* A **349** 236–47
[144] Fan Y M, Guo H, Xu J, Chu K, Zhu X X and Jia C C 2011 Effects of boron on the microstructure and thermal properties of Cu/diamond composites prepared by pressure infiltration *Int. J. Miner. Metall. Mater.* **18** 472–8
[145] Sinha V and Spowart J E 2013 Influence of interfacial carbide layer characteristics on thermal properties of copper-diamond composites *J. Mater. Sci.* **48** 1330–41
[146] Fei W D, Hu M and Yao C K 2003 Thermal expansion and thermal mismatch stress relaxation behaviors of SiC whisker reinforced aluminum composite *Mater. Chem. Phys.* **77** 882–8
[147] Sharma N K, Misra R K and Sharma S 2016 Modeling of thermal expansion behavior of densely packed Al/SiC composites *Int. J. Solids Struct.* **102–103** 77–88
[148] Gad S I, Attia M A, Hassan M A and El-Shafei A G 2021 A random microstructure-based model to study the effect of the shape of reinforcement particles on the damage of elastoplastic particulate metal matrix composites *Ceram. Int.* **47** 3444–61
[149] Gao X, Zhang X X and Geng L 2019 Strengthening and fracture behaviors in SiCp/Al composites with network particle distribution architecture *Mater. Sci. Eng.* A **740–741** 353–62
[150] Li J C, Chen X W and Huang F L 2018 On the mechanical properties of particle reinforced metallic glass matrix composites *J. Alloys Compd.* **737** 271–94
[151] Wu Q, Xu W X and Zhang L C 2019 Microstructure-based modelling of fracture of particulate reinforced metal matrix composites *Composites* B **163** 384–92
[152] Liu N, Zhang Q Q, Zhang H Y, Cao F, Feng P F, Zuo Y F, Jiang Y H, Tang W T and Liang S H 2022 Experimental verification and numerical analysis on plastic deformation and mechanical properties of the *in-situ* TiB_2 homogeneous composites and TiB_2/Cu network composites prepared by powder metallurgy *J. Alloys Compd.* **920** 165897
[153] Zhang J, Ouyang Q B, Guo Q, Li Z Q, Fan G F, Zuo Y F, Jiang Y H, Tang W T and Liang S H 2016 3D microstructure-based finite element modeling of deformation and fracture of SiCp/Al composites *Compos. Sci. Technol.* **123** 1–9
[154] Karadeniz Z H and Kumlutas D 2007 A numerical study on the coefficients of thermal expansion of fiber reinforced composite materials *Compos. Struct.* **78** 1–10
[155] Davis L C and Artz B E 1995 Thermal conductivity of metal-matrix composites *J. Appl. Phys.* **77** 4954–60
[156] León-Patiño C A, Braulio-Sánchez M, Aguilar-Reyes E A and Bedolla-Becerril E 2019 Microstructure, mechanical and thermal properties of Ni matrix composites reinforced with high-volume TiC *J. Alloys Compd.* **792** 1102–11
[157] Chen G Q, Yang W S, Dong R H, Hussain M and Wu G H 2014 Interfacial microstructure and its effect on thermal conductivity of SiCp/Cu composites *Mater. Des.* **63** 109–14
[158] Molina J M, Prieto R, Narciso J and Louis E 2009 The effect of porosity on the thermal conductivity of Al-12wt.% Si/SiC composites *Scr. Mater.* **60** 582–5
[159] Chu K, Jia C C, Liang X B, Chen H and Guo H 2009 The thermal conductivity of pressure infiltrated SiC_p/Al composites with various size distributions: experimental study and modeling *Mater. Des.* **30** 3497–503
[160] Fu X L, Hu Y B, Peng G and Tao J 2017 Effect of reinforcement content on the density, mechanical and tribological properties of Ti_3SiC_2/Al_2O_3 hybrid reinforced copper-matrix pantograph slide *Sci. Eng. Compos. Mater.* **24** 807–15
[161] Wei H M, Zou J P, Gong Y R, Li X Y, Zhan W Y and Li F Y 2022 Effects of Ti_2SnC on the mechanical properties and tribological properties of copper/graphite composites *Ceram. Int.* **48** 36853–9
[162] Ngai T L, Zheng W and Li Y Y 2013 Effect of sintering temperature on the preparation of Cu–Ti_3SiC_2 metal matrix composite *Prog. Nat. Sci.: Mater. Int.* **23** 70–76
[163] Zhang J, Wang J Y and Zhou Y C 2007 Structure stability of Ti_3AlC_2 in Cu and microstructure evolution of Cu–Ti_3AlC_2 composites *Acta Mater.* **55** 4381–90
[164] Huang X C, Feng Y, Qian G, Zhao H, Zhang J C and Zhang X B 2018 Physical, mechanical, and ablation properties of Cu–Ti_3AlC_2 composites with various Ti_3AlC_2 contents *Mater. Sci. Technol.* **34** 757–62
[165] Liu Y, Tang X H, Zhou S F, Guo B S, Zhang Z G and Li W 2022 Improving mechanical properties of Cu/Ti_3AlC_2 composites via *in-situ* decomposed gradient interfaces *Mater. Sci. Eng.* A **834** 142615
[166] Salvo C, Chicardi E, Hernández-Saz J, Aguilar C, Gnanaprakasam P and Mangalaraja R V 2021 Microstructure, electrical and mechanical properties of Ti_2AlN MAX phase reinforced copper matrix composites processed by hot pressing *Mater. Charact.* **171** 110812
[167] Jahani A, Jamshidi Aval H, Rajabi M and Jamaati R 2022 Effects of Ti_2SnC MAX phase on microstructure, mechanical, electrical, and wear properties of stir-extruded copper matrix composite *Adv. Eng. Mater.* **25** 2201463
[168] Zhang R, Chen B, Liu F Y, Sun M, Zhang H M and Wu C L 2022 Microstructure and mechanical properties of composites obtained by spark plasma sintering of Ti_3SiC_2-15 vol.%Cu mixtures *Materials* **15** 2515
[169] Fathy A, Wagih A and Abu-Oqail A 2019 Effect of ZrO_2 content on properties of Cu-ZrO_2 nanocomposites synthesized by optimized high energy ball milling *Ceram. Int.* **45** 2319–29
[170] Nan L, Xi Z, Qiangqiang Z, Yihui J, Yishi S, Qian L, Pengfa F, Wenting T and Shuhua L 2022 Numerical evaluation and experimental verification of mechanical properties and fracture behavior for TiB_2/Cu composites prepared by *in-situ* mixing casting *J. Alloys Compd.* **895** 162475
[171] Shen M J, Wang X J, Ying T, Wu K and Song W J 2016 Characteristics and mechanical properties of magnesium matrix composites reinforced with micron/submicron/nano SiC particles *J. Alloys Compd.* **686** 831–40
[172] Zhang L J, Qiu F, Wang J G, Wang H Y and Jiang Q C 2015 Microstructures and mechanical properties of the Al2014 composites reinforced with bimodal sized SiC particles *Mater. Sci. Eng.* A **637** 70–74
[173] Shen M J, Wang X J, Zhang M F, Zheng M Y and Wu K 2015 Significantly improved strength and ductility in bimodal-size grained microstructural magnesium matrix composites reinforced by bimodal sized SiCp over traditional magnesium matrix composites *Compos. Sci. Technol.* **118** 85–93
[174] Tian W S, Zhao Q L, Geng R, Qiu F and Jiang Q C 2018 Improved creep resistance of Al-Cu alloy matrix

composite reinforced with bimodal-sized TiC_p *Mater. Sci. Eng.* A **713** 190–4
[175] Tian W S, Zhao Q L, Zhang Q Q, Qiu F and Jiang Q C 2018 Enhanced strength and ductility at room and elevated temperatures of Al-Cu alloy matrix composites reinforced with bimodal-sized TiC_p compared with monomodal–sized TiC_p *Mater. Sci. Eng.* A **724** 368–75
[176] Ma S M, Zhuang X C and Wang X M 2019 3D micromechanical simulation of the mechanical behavior of an *in-situ* Al_3Ti/A356 composite *Composites* B **176** 107115
[177] Yan Y W, Geng L and Li A B 2007 Experimental and numerical studies of the effect of particle size on the deformation behavior of the metal matrix composites *Mater. Sci. Eng.* A **448** 315–25
[178] Wang C C, Min G H and Kang S B 2009 Electrical behavior of SiCp reinforced copper matrix composites by hot pressing *Adv. Mater. Res.* **79–82** 1579–82
[179] Geng L and Yan Y W 2007 Effects of particle size on the thermal physical properties of SiC_p/Al composites *Key Eng. Mater.* **351** 131–4
[180] Elomari S, Skibo M D, Sundarrajan A and Richards H 1998 Thermal expansion behavior of particulate metal-matrix composites *Compos. Sci. Technol.* **58** 369–76
[181] Efe G C, Ipek M, Zeytin S and Bindal C 2012 An investigation of the effect of SiC particle size on Cu-SiC composites *Composites* B **43** 1813–22
[182] Xuan Q Q, Shu S L, Qiu F, Jin S B and Jiang Q C 2012 Different strain-rate dependent compressive properties and work-hardening capacities of 50vol% TiC_x/Al and TiB_2/Al composites *Mater. Sci. Eng.* A **538** 335–9
[183] Meijer G, Ellyin F and Xia Z 2000 Aspects of residual thermal stress/strain in particle reinforced metal matrix composites *Composites* B **31** 29–37
[184] Chen C R, Qin S Y, Li S X and Wen J L 2000 Finite element analysis about effects of particle morphology on mechanical response of composites *Mater. Sci. Eng.* A **278** 96–105
[185] Liu N, Zhang X, Zhang X D, Feng P F, Zuo Y F, Cao F, Su Y S, Jiang Y H and Liang S H 2022 Numerical investigations on the hybrid effect and deformation mechanism of TiB_{2p} and TiB_w reinforced Cu composites prepared by *in-situ* mixing casting *Comput. Mater. Sci.* **213** 111657
[186] Chmielewski M, Pietrzak K, Teodorczyk M, Nosewicz S, Jarząbek D, Zybała R, Bazarnik P, Lewandowska M and Strojny-Nędza A 2017 Effect of metallic coating on the properties of copper-silicon carbide composites *Appl. Surf. Sci.* **421** 159–69
[187] Yang H Y, Yan Y F, Liu T S, Dong B X, Chen L Y, Shu S L, Qiu F, Jiang Q C and Zhang L C 2021 Unprecedented enhancement in strength-plasticity synergy of (TiC+Al_6MoTi+Mo)/Al cermet by multiple length-scale microstructure stimulated synergistic deformation *Composites* B **225** 109265
[188] Yan Y F, Kou S Q, Yang H Y, Dong B X, Shu S L, Chen L Y, Qiu F and Zhang L C 2023 Manipulating interface bonding and microstructure via tuning interfacial reaction for enhancing mechanical property of *in-situ* TiC/Al cermets *J. Mater. Process. Technol.* **317** 117995
[189] Hu Y B and Cong W L 2018 A review on laser deposition-additive manufacturing of ceramics and ceramic reinforced metal matrix composites *Ceram. Int.* **44** 20599–612
[190] Mitra R and Mahajan Y R 1995 Interfaces in discontinuously reinforced metal matrix composites: an overview *Bull. Mater. Sci.* **18** 405–34
[191] Yang H Y, Wang Z, Chen L Y, Shu S L, Qiu F and Zhang L C 2021 Interface formation and bonding control in high-volume-fraction (TiC+TiB_2)/Al composites and their roles in enhancing properties *Composites* B **209** 108605
[192] Zhao C and Wang J 2013 Enhanced mechanical properties in diamond/Cu composites with chromium carbide coating for structural applications *Mater. Sci. Eng.* A **588** 221–7
[193] Weber L and Tavangar R 2007 On the influence of active element content on the thermal conductivity and thermal expansion of Cu-X (X = Cr, B) diamond composites *Scr. Mater.* **57** 988–91
[194] Zhang C C, Luo G Q, Zhang J, Dai Y, Shen Q and Zhang L M 2017 Synthesis and thermal conductivity improvement of W-Cu composites modified with WC interfacial layer *Mater. Des.* **127** 233–42
[195] Zhang L, Qu X H, Duan B H, He X B, Ren S B and Qin M L 2009 Thermal expansion behaviour of SiC_p/Cu composites prepared by spark plasma sintering and pressureless infiltration *Powder Metall.* **52** 17–23
[196] Wang Y, Xu Y H, Cao Z Y, Yan C, Wang K, Chen J J, Cheng S Y and Feng Z S 2019 A facile process to manufacture high performance copper layer on ceramic material via biomimetic modification and electroless plating *Composites* B **157** 123–30
[197] Tian Y N, Dou Z H, Niu L P and Zhang T A 2019 Studies on copper-coated boron carbide particle-reinforced copper-matrix/graphite self-lubricating composite materials *Russ. J. Non-Ferr. Met.* **60** 575–82
[198] Xiang S Q, Du X J, Liang Y H, Zhou M C and Zhang X F 2021 Optimizing phase interface of titanium carbide-reinforced copper matrix composites fabricated by electropulsing-assisted flash sintering *Mater. Sci. Eng.* A **819** 141506